Direct observation of fluorescent proteins in gels: a rapid cost-efficient, and quantitative alternative to immunoblotting

Matthieu Sanial[1], Ryan Miled[1], Marine Alves[1], Sandra Claret[1], Nicolas Joly[1], Véronique Proux-Gillardeaux[1], Anne Plessis[1], Sébastien Léon[1,2]

Affiliations:

[1] : Université Paris Cité, CNRS, Institut Jacques Monod, F-75013, Paris, France.

[2] : Author for correspondence:

Sébastien Léon, PhD

Institut Jacques Monod

15 Rue Hélène Brion

75205 Paris cedex 13, France.

email: sebastien.leon@ijm.fr ; tel. +33 (0)1 57 27 80 57.

Running title:

In-gel fluorescence detection of fluorescent proteins as an alternative to immunoblotting

Abstract

The discovery of Green Fluorescent Protein (GFP) and its derivatives has revolutionized cell biology. These fluorescent proteins (FPs) have enabled the real-time observation of protein localization and dynamics within live cells. Applications of FP vary from monitoring gene/protein expression patterns, visualizing protein-protein interactions, measuring protein stability, assessing protein mobility and creating biosensors. The utility of FPs also extends to biochemical approaches through immunoblotting and proteomic analyses, aided by anti-FP antibodies and nanobodies. FPs are notoriously robust proteins with a tightly folded domain that confers a strong stability and a relative resistance to degradation and denaturation. In this study, we report that various green and red FPs can be maintained in a native, fluorescent form during the entire process of protein sample extraction, incubation with sample buffer, loading and migration on SDS-PAGE with only minor adaptations of traditional protocols. This protocol results in the ability to detect and quantify in-gel fluorescence (IGF) of endogenously-expressed proteins tagged with FPs directly after migration, using standard fluorescence-imaging devices. This approach eliminates the need for antibodies and chemiluminescent reagents, as well as the time-consuming steps inherent to immunoblotting such as transfer onto a membrane and antibody incubations. Overall, IGF detection provides clearer data with less background interference, a sensitivity comparable or better to antibody-based detection, a better quantification and a broader dynamic range. After fluorescence imaging, gels can still be used for other applications such as total protein staining or immunoblotting if needed. It also expands possibilities by allowing the detection of FPs for which antibodies are not available. Our study explores the feasibility, limitations, and applications of IGF for detecting endogenously expressed proteins in cell extracts, providing insights into sample preparation, imaging conditions, and sensitivity optimizations, and potential applications such as co-immunoprecipitation experiments.

Introduction

The development of GFP as a tool to study protein localization and dynamics in live cells has been a revolution in the field of cell biology, as recognized by the Nobel prize in Chemistry awarded in 2008 to Osamu Shimomura, Martin Chalfie and Roger Tsien (Chalfie et al., 1994; Tsien, 1998). GFP and its derivatives, as well as other fluorescent proteins (FPs) isolated since then from other organisms with various properties (Lambert, 2019; Shaner et al., 2005), have become instrumental in many fields of biology. They allow to monitor protein expression and localization in live cells, and can be used as reporters of gene/protein expression patterns in organisms or tissues. Various techniques have been implemented using GFP and its variants to visualize protein-protein interactions in cells, through bimolecular fluorescence complementation (Hu and Kerppola, 2003; Romei and Boxer, 2019), or fluorescence resonance energy transfer (FRET, BRET) (Hochreiter et al., 2015). This also opened the way to the development of various probes and biosensors to report on the quantity and/or localization of ions, metabolites and other organic molecules in cells and tissues (Chandris et al., 2021; Wang et al., 2023; Zacharias et al., 2002). The various folding kinetics of FPs have been exploited to report on protein stability and half-life (fluorescent timers) (Khmelinskii et al., 2012; Subach et al., 2009; Terskikh et al., 2000). The fact that fluorescence bleaches upon intense illumination also provides a way to evaluate protein mobility and dynamics in live cells (Fluorescence Recovery after Photobleaching [FRAP] and Fluorescence Loss in Photobleaching [FLIP]) (White and Stelzer, 1999). Similarly, photo-activatable and photo-switchable FPs allow the study of distinct protein pools over time by activating or converting their fluorescence upon illumination (Wang et al., 2023). Following the development of robust anti-GFP antibodies and in particular of nanobodies (Rothbauer et al., 2006), GFP can also be used like any other epitope for protein detection by techniques ranging from immunoblotting to immunoprecipitation and proteomic analyses (Cristea et al., 2005; Rothbauer et al., 2008). Finally, the ability to express a GFP-binding protein (derived from a llama single chain antibody) in cells fused with cellular proteins provides a way to modify the subcellular localization and interactions of a GFP-tagged protein at will (Rothbauer et al., 2008).

Because of these many applications, GFP and other FPs are frequently used as protein tags in cell biology studies. An early step in the workflow consists in verifying the expression of an intact fusion protein in cells by immunoblotting. Immunoblotting is also required when GFP is used as any epitope to monitor the fusion protein's integrity, stability or post-translational modifications, or in interaction studies based on co-immunoprecipitations. Protein detection by immunoblotting involves primary antibodies and most generally a chemiluminescent reaction (ECL) using secondary antibodies coupled to an enzyme (horseradish peroxidase). Whereas this approach is considered to be more sensitive, enzyme kinetics may interfere with the linearity of the signal vis-à-vis the amount of detected protein, a problem that may hinder the quantification of signals.

Over the past 20 years, fluorescent alternatives to chemiluminescence-based protein detection were introduced, and the development of fluorescent dyes and the amelioration of fluorescence-based imaging systems have allowed for a better sensitivity and better quantification of signals (Eaton et al., 2014). Although initial systems focused on fluorescence detection at high wavelengths (far-red and infrared, i.e. around 700 nm and above) to minimize background autofluorescence, commercial imaging systems now allow the visualization of fluorescence at additional wavelengths compatible with usual commercial fluorophores, eg. those used for immunofluorescence.

The versatility of these imaging systems is such that, in principle, the endogenous fluorescence of the widely used FPs (eg. GFP) in extracts could be monitored directly in gels without the need of transfer to membrane or the use of antibodies. SDS-PAGE involves denaturation of protein samples at high temperatures in the presence of SDS and reducing agents prior to loading onto a gel, procedures that are usually considered incompatible with the maintenance of FP fluorescence in gel (Chew et al., 2009). A few studies have reported the observation of GFP-fluorescence in gels, but these approaches require the use of native PAGE (Nemec et al., 2017), which has drawbacks compared to regular, denaturing SDS-PAGE. On the other hand, GFP and FPs in general are known to be tightly folded and more resistant to denaturation than most proteins (Saeed and Ashraf, 2009; Ward, 2005). For example, a few studies exploited the ability of GFP to resist the adverse conditions of SDS-PAGE to run protein overexpression screens in *Escherichia coli* or other cell types (Bird et al., 2015; Bomholt et al., 2013; Geertsma et al., 2008; Krasnoselska et al., 2021; Madani et al., 2021; Muller-Lucks et al., 2012; Newstead et al., 2007), or on recombinantly expressed or purified proteins *in vitro* (Campbell et al., 2002; Donate-Macian et al., 2019; Nakatani et al., 2019; Weinberger Ii and Lennon, 2021).

The development and popularity of fluorescence imaging devices is likely to lead to a generalization of the use of FPs for direct visualization of in-gel fluorescence (IGF). Accordingly, a recent study used this method for easy detection of FP-tagged proteins in protein extracts of cell culture (Ruan et al., 2023).

In this study, we document that in-gel fluorescence (IGF) detection is a rapid and cost-effective alternative to immunoblotting to visualize FP-tagged proteins expressed at endogenous levels in cell extracts. IGF avoids the time-consuming process of transfer to a membrane, incubations with antibodies and washes, with substantial improvements of the cost of the experiment as this does not require primary nor secondary antibodies, membranes, or chemiluminescence substrates, and of the quality of the data (less background and higher dynamic range). We describe the conditions of use and limitations of various GFPs and RFPs for IGF, as well as sample preparation, imaging conditions, sensitivity and possible applications.

Results

The fluorescence of endogenously yeGFP-tagged proteins can be visualized from cell extracts in SDS-PAGE gel after migration

To know whether we can detect GFP fluorescence from endogenously expressed proteins in total protein extracts, we tagged two yeast genes (*BMH1*, encoding a 14-3-3 protein) or HXK1, encoding hexokinase 1) at their endogenous locus with yeGFP, a yeast codon-optimized GFP (Cormack et al., 1997) which also harbors two mutations (S65G, S72A - a.k.a. “GFPmut 3”, Cormack et al., 1996) selected to increase GFP fluorescence (ID on FPBase https://www.fpbase.org : A2OWC, Lambert, 2019). yeGFP is often used for fluorescent tagging as it is incorporated into a toolbox for PCR-based tagging of yeast genes at their endogenous genetic locus (Janke et al., 2004). Exponentially growing cells (5 OD equivalents) were lysed with glass beads at 4°C in 100 µL native lysis buffer (containing Tris-HCl, Triton X-100 and NaCl; see Material and Methods for more details). 4X Laemmli sample buffer (Bio-Rad, containing LDS and DTT) was then added to the lysates (1X final), and samples were then incubated at 30°C or 95°C for 5 min, before loading on commercial precast TGX gels, and run in Tris-Glycine-SDS (TGS) buffer. After migration, the gel was imaged with gel-imaging devices whose excitation/emission wavelengths were compatible with the observation of green fluorescent proteins (ChemiDoc MP, Bio-Rad: 460-490/518-546 nm; and Typhoon, Cytiva: 488/505-545 nm) (**Figure S1**). The gels displayed a green fluorescent signal at the size of the tagged proteins, as revealed by immunoblotting with anti-GFP antibodies after transfer of the same gel to a membrane (**Figure 1A**). Thus, at least some of the GFP molecules remained fluorescent throughout the sample preparation and gel migration process. Noteworthy, other lysis buffers were tested and also allowed the maintenance of GFP fluorescence (see Material and Methods for more details). On a side note, we observed that gel exposure to UV-light (such as during total protein labeling with a trihalo compound, eg. “Stain-Free” technology from Bio-Rad: 45 sec exposure at 300-400 nm) partially bleached the GFP fluorescence signal (**Figure S2**). Thus, this labeling should preferentially be performed after visualizing the GFP signal, especially if the signal is weak. Finally, as expected, GFP was no longer fluorescent when samples were denatured at 95°C instead of 30°C, or when extracts were prepared from cells precipitated with TCA in which proteins are fully denatured (**Figure 1A**).

Whereas these mild denaturing conditions allow the detection of in-gel fluorescence, two important points should be noted. First, the lower level of denaturation can impact on the migration of the GFP-tagged protein. At 30°C, Bmh1-yeGFP and Hxk1-yeGFP migrated faster than when samples were heated at 95°C or precipitated with TCA, as determined after transfer and immunoblotting with anti-GFP antibodies (**Figure 1A**). In-gel fluorescence detection systematically correlated with the presence of the fast-migrating band, suggesting it may correspond to a folded species of yeGFP. To address this point, proteins were transferred onto a nitrocellulose membrane

132 in classical conditions (liquid transfer), and immunoblotted with anti-GFP antibodies. Bmh1-yeGFP
133 fluorescence signal could be detected on the nitrocellulose membrane even after transfer and
134 incubation with antibodies, allowing the sequential observation of yeGFP fluorescence and antibody-
135 based labeling during the same acquisition. This revealed that the yeGFP fluorescence signal
136 precisely overlaid with the fast-migrating band detected with the anti-GFP antibody (**Figure 1B**).
137 Thus, yeGFP remains mostly folded in these mild denaturation conditions allowing in-gel
138 fluorescence observation, but can also cause a variation in the apparent molecular weight of yeGFP-
139 tagged proteins as compared to denatured proteins.

140 A second aspect that should be considered when using low denaturing conditions is that various
141 antibodies may recognize folded and denatured fluorescent proteins with different affinities. For
142 instance, anti-GFP antibodies may display a greater affinity towards folded or unfolded GFP, leading
143 to potential artifacts during quantification of the signal (**Figure S3A**). This could be circumvented by
144 denaturing proteins directly on the membrane after transfer (**Figure S3B**, see Material and Methods).

145 Comparison of GFP(S65T), yeGFP and EGFP for in-gel fluorescence 146 visualization

147 Following the development of tools for tagging of yeast genes with various tags by homologous
148 recombination (Longtine et al., 1998; Wach et al., 1997), Huh et al. generated a collection of yeast
149 strains which is widely used by the community and in which most genes are individually tagged with
150 GFP(S65T) (Huh et al., 2003) (FPBase ID: B6J33). To evaluate whether strains from this collection
151 are suitable for in-gel fluorescence detection, we retrieved the Bmh1-GFP(S65T) strain and
152 subjected it to the same analysis. A fluorescent signal was detected in the gel when samples were
153 incubated at 30°C, but not 95°C (**Figure 2A**). When compared to the signal obtained when tagging
154 the same protein with yeGFP, the fluorescent signal observed with GFP(S65T) was weaker,
155 probably because GFP(S65T) was less robust and more prone to denaturation. Indeed, a large
156 fraction of the Bmh1-GFP(S65T) protein pool was denatured even when incubated at 30°C prior to
157 gel loading, as judged by the migration pattern revealed with anti-GFP antibodies and antibodies
158 directed to the proteins of interest (**Figure 2A**). Thus, GFP(S65T) is subject to a partial denaturation
159 even in conditions which otherwise preserve yeGFP fluorescence. This was confirmed when
160 comparing the staining of Hxk1-GFP(S65T) with that of Hxk1-yeGFP (**Figure 2A**). In conclusion,
161 fusions with GFP(S65T) (including those from the GFP collection, Huh et al., 2003) are not the best-
162 suited to detect in-gel fluorescence in our conditions.

163 We also tested another commonly used GFP variant, EGFP, which derives from the original
164 avGFP and carries mutations F64L and S65T (a.k.a. “GFPmut 1”, FPBase ID: R9NL8, Cormack et
165 al., 1996). This variant is also commonly used for the tagging of yeast genes at their endogenous
166 genetic locus (Janke et al., 2004) and is widely used in other eukaryotic organisms, notably through
167 their availability in the pEGFP-N1/pEGFP-C1 plasmids for expression in mammalian cells. The

168 signals obtained with EGFP were comparable to those obtained for yeGFP, making it appropriate
169 for visualization of IGF (**Fig 2B**).

170 In-gel fluorescence detection of proteins tagged with mNeonGreen and 171 superfolder GFP

172 We next tested the suitability of more recently developed green-fluorescent proteins for IGF
173 detection (**Figure 3**). For comparative purposes, the same protein that we used for the initial variants
174 tested, Bmh1, was tagged with the brighter dLanYFP-derivative, mNeonGreen (FPBase ID: ZRKRV,
175 Shaner et al., 2013) or with superfolder GFP (sfGFP), a tightly folded GFP which is even more
176 resistant to denaturation than traditional GFP (FPBase ID: B4SOW, Pedelacq et al., 2006).
177 In all cases, a fluorescent signal was detected in the gel when samples were incubated at 30°C
178 prior to loading (**Figure 3**). Various fluorescence intensities were observed, with the strongest signal
179 obtained for Bmh1-yeGFP. However, these variations could be due to (i) the spectral properties of
180 these fluorescent proteins which may not appropriately match the imaging systems used for their
181 detection, (ii) the ability of these fluorescent proteins to endure the sample preparation conditions
182 and SDS-PAGE protocol, and (iii) an effect of the tag on the expression level of the tagged protein
183 (**Figure 3**). Indeed, in our experiments, Bmh1-yeGFP was more highly expressed than Bmh1-
184 mNeonGreen or Bmh1-sfGFP, as determined by immunoblotting these proteins with anti-Bmh1
185 antibodies. We hypothesized that this lower level of expression might be due to the fact that only
186 Bmh1-yeGFP is codon-optimized for expression in yeast. However, optimizing codon usage for
187 mNeonGreen expression in yeast (ymNeonGreen) neither led to an increase in protein expression
188 nor in IGF signal (**Figure S4**). This hypothesis remains open for sfGFP, as we did not test
189 optimization of codon usage for this FP.
190 The loss of IGF signal upon denaturation at 95°C was accompanied by a change in the migration
191 pattern as revealed by western blotting using anti-Bmh1 antibodies, with only one band present at a
192 higher apparent molecular weight, corresponding to the non-fluorescent species. An intermediate
193 situation was observed upon denaturation at 50°C, with a decrease in Bmh1-mNeonGreen IGF,
194 unlike what was observed for Bmh1-yeGFP or sfGFP (**Figure 3**). Accordingly, by immunoblotting,
195 treatment of samples at 50°C led to an almost full conversion of Bmh1-mNeonGreen from the native
196 to the denatured form, which was less pronounced for Bmh1-yeGFP. Thus, mNeonGreen is
197 amenable to IGF detection but is less heat-stable than other green FPs. In contrast, Bmh1-sfGFP
198 migration was unaffected at 50°C compared to 30°C, highlighting the stronger heat-stability of this
199 fluorescent variant. Overall, we conclude that sfGFP and EGFP (see **Figure 2B**) are more resistant
200 to heat-induced denaturation than yeGFP, GFP(S65T) and mNeonGreen.
201 These observations led us to quantify the heat-stability of fluorescence of the most robust green
202 FPs, which could be helpful for applications in which samples must be incubated at temperatures
203 higher than 30°C. We determined in-gel fluorescence as a function of the denaturation temperature
204 (**Figure 4**). In-gel fluorescence of Bmh1-sfGFP was unaltered until reaching 59°C, whereas Bmh1-

205 yeGFP fluorescence decreased starting at 54°C (**Figure 4A, C-D**). The temperature at which 50%
206 of the signal is still present was 67°C for sfGFP and 59°C for yeGFP. Interestingly, EGFP behaved
207 similarly to sfGFP (**Figure 4B, D**). The only additional gain of tagging with sfGFP over the widely
208 used EGFP is that it migrates almost exclusively as a single band at low denaturing temperatures
209 (30°C). Again, denaturation of all green FP-tagged Bmh1 was accompanied by a decrease in its
210 mobility on gels, which could clearly be visualized using anti-Bmh1 antibodies (**Figure 4, A-C**).
211 Altogether, these results allow us to reach the following conclusions. First, Bmh1-yeGFP and
212 Bmh1-EGFP give a strong IGF signal that, in our experiments, could be attributed to a higher
213 expression level coupled to a relatively high resistance to denaturation, especially in the case of
214 EGFP. Indeed, EGFP was as resistant as sfGFP to heat-induced denaturation in our conditions.
215 Second, despite being more sensitive to the conditions of extraction and imaging, mNeonGreen in-
216 gel fluorescence can still be used at low denaturation temperatures, which can avoid the purchase
217 of specific antibodies – indeed, mNeonGreen shares only 25% identity with the traditional avGFP
218 and is not recognized by anti-GFP antibodies. Finally, care should be taken regarding the expression
219 level of the tagged protein which, despite tagging at the endogenous genetic locus, can lead to
220 strong variations in expression depending on which FP was used for tagging (see **Figure 3**).

221 In-gel fluorescence of red fluorescent proteins

222 We aimed at expanding our observations to other, non-green fluorescent proteins. We could
223 not test blue-fluorescent proteins because none of the commonly-used imaging devices (Chemidoc
224 MP and Typhoon) provide filters compatible with the excitation/emission spectra of blue-fluorescent
225 proteins. However, these experiments were possible for red-fluorescent proteins. We tagged Bmh1
226 with the widely used fluorescent protein mCherry, a monomeric DsRed derivative with many
227 advantages such as high photostability, faster maturation and high pH-stability (FPBase ID: ZERB6,
228 Shaner et al., 2004). We also fused Bmh1 with mRuby2, a bright derivative of eqFP611 (FPBase ID:
229 8MJ78, Lam et al., 2012) , and with TagRFP-T, which derives from eqFP578 (Merzlyak et al., 2007)
230 with enhanced photostability (FPBase ID: LF3LJ, Shaner et al., 2008). Protein extracts were run on
231 SDS-PAGE and in-gel fluorescence was observed at excitation/emission wavelengths of 532/550-
232 800nm (Typhoon) or 520-545/577-613nm (ChemiDoc MP). All samples gave a red fluorescent signal
233 in gel (**Figure 5A**). Fluorescence signals were globally stronger when using a long-pass filter on the
234 Typhoon (550-800nm), which collects more fluorescence signals than the narrower filter present on
235 the Chemidoc MP (577-613nm) (**Figure S5**). The strongest fluorescence signal was obtained for
236 Bmh1-mCherry, whereas Bmh1-TagRFP-T gave the weakest signal. Immunoblotting using anti-
237 Bmh1 antibodies revealed migration patterns comparable to those obtained for green fluorescent
238 proteins: a faster-migrating band corresponded to the fluorescent species, whereas the slower
239 migrating form corresponded to the denatured pool. The ratio of fluorescent over denatured proteins
240 was higher for mCherry, although a minor denatured pool was already present in mild denaturing
241 conditions. Notably, the fluorescent pool of Bmh1-mRuby2 migrated much faster than any other FP-

242 tagged Bmh1 protein, with a decrease of about 15 kDa in apparent MW compared to the denatured
243 version. Bmh1-mCh was also the best detected red fluorescent protein on the Chemidoc MP (**Figure**
244 **5A**). Altogether, our conclusions are that (i) mild denaturation conditions are compatible with IGF of
245 RFPs, with mCherry being the best tag in our hands, with a stronger signal and resistance to heat-
246 induced denaturation; (ii) IGF allows the visualization of proteins tagged with RFPs originating from
247 various organisms without the need to purchase specific antibodies; (iii) tagging of proteins with red
248 FPs can lead to significant changes in the apparent molecular weight of the fusion proteins in mild
249 denaturing conditions.

250 Because mCherry is a widely used FP and is the most fluorescent of all RFPs tested, we then
251 evaluated the resistance of Bmh1-mCh to temperature-induced denaturation (**Figure 5, B-C**).
252 mCherry fluorescence was maintained at up to 70°C, with 50% of the signal still being present at
253 79°C. Thus, of all FPs tested (including green FPs), mCherry is the most resistant to denaturation
254 and is therefore perfectly appropriate for IGF signal detection.

255 Linearity of the signal and sensitivity of IGF compared to immunoblotting-
256 based chemiluminescence detection

257 Having established the capacity to detect fluorescence of numerous FPs in gels, we then turned
258 to studying the linearity of the signal and the sensitivity of this approach compared to the traditional
259 immunoblotting approach. When serial dilutions of Bmh1-yeGFP samples were initially assayed, we
260 discovered that the simple dilution of the protein lysate in Laemmli buffer (containing SDS and DTT)
261 was sufficient to promote FP denaturation, as determined by examining the migration profile using
262 anti–Bmh1 antibodies. This was likely a consequence of an increase in the detergent/protein ratio,
263 as previously observed (Xu and Keiderling, 2004) (**Figure S6**). To circumvent this problem, we
264 repeated the experiment using a non-denaturing sample buffer for dilutions of the sample (Laemmli
265 buffer without LDS). Under these conditions, protein fluorescence was maintained in spite of the
266 dilution (**Figure 6**).

267 In-gel fluorescence was compared to the signal obtained using primary antibodies followed by
268 secondary antibodies coupled to horseradish peroxidase (HRP) for chemiluminescent detection. We
269 used either antibodies raised against Bmh1 (**Figure 6A**) or GFP (**Figure 6B**). Overall, IGF detection
270 was comparable or better in sensitivity to chemiluminescent detection. This was particularly true
271 when comparing IGF with anti-GFP-based detection. Overall, we found the fluorescent signal to
272 more closely follow a linear plot than the chemiluminescent signal, over a range of 320-fold (**Figure**
273 **6B**). This result was confirmed for all FPs we tested, including mCherry (**Figure S7**). Thus, we
274 conclude that IGF detection is more reliable than chemiluminescent detection.

275 ## Increasing the pH protects against FP denaturation at low protein
276 concentrations

277 Our observations above (**Figure S6**) suggested that sample dilution in Laemmli buffer
278 compromises the integrity of GFP. Although we observed that this could be circumvented by the use
279 of detergent-free Laemmli buffer (**Figure 6**), we sought to find conditions in which sample dilution
280 would maintain FP integrity despite the presence of detergent (**Figure 7A**). First, we observed that
281 dilution of the protein lysate in native lysis buffer (Tris-HCl 100 mM pH 8.0, NaCl 0.15 M, Glycerol
282 5%, Triton X-100 0.5 %) instead of water (**Figure 7A**) led to a protection of fluorescence, as
283 determined both by IGF detection and the observation of native/denatured species by
284 immunoblotting (**Figure 7B**). This result could partially be attributed to the presence of NaCl in the
285 native lysis buffer, which preserved fluorescence in itself (**Figure 7B**). Moreover, increasing the pH
286 to 8.0 or above was sufficient to protect fluorescence at low protein concentrations (**Figure 7C**),
287 allowing IGF detection even for diluted protein samples. We conclude that increasing the sample pH
288 to pH 8.0 protects GFP denaturation in diluted samples.

289 ## Use of IGF for the detection of FP-tagged proteins interaction by co-
290 immunoprecipitation

291 We sought to exploit the power of IGF detection in a situation in which two fluorescent proteins
292 must be detected. Protein-protein interactions can be studied by the co-expression of tagged
293 proteins and immunoprecipitation of one partner to reveal the presence of the potential partner in
294 the immunoprecipitate. As a case study, we studied the interaction between the yeast 14-3-3
295 proteins Bmh1 and Bmh2, which are known to heterodimerize *in vivo* (Chaudhri et al., 2003). Lysates
296 of yeast expressing Bmh1-yeGFP and Bmh2-ymCh (a yeast codon–optimized version of mCherry,
297 see Material and Methods) were subjected to immunoprecipitation using nanobodies-based traps.
298 Similarly to our observations on diluted samples (section above), we realized that
299 immunoprecipitates of FP proteins were denatured in the presence of Laemmli buffer, likely because
300 of the low protein concentration in these samples. Based on our findings above (**Figure 7**),
301 immunoprecipitates were resuspended in Laemmli buffer at pH 8.0 before loading, and samples
302 were migrated on SDS-PAGE and imaged for IGF. In both cases (GFP-trap: **Figure 8A**; RFP-trap:
303 **Figure 8B**), IGF detection allowed detection of both the bait and the prey on the same gel after
304 exposure to the appropriate wavelengths, within minutes after uncasting the gel. One limitation was
305 a bleed-through of intense green fluorescence signals in the red channel, which was notably
306 observed using the Chemidoc (**Figure S8**) but also using the Typhoon to a limited extent (**Figure 8**).
307 Thus, when looking at proteins tagged in both channels, the size of the green fluorescence-tagged
308 protein should be different from that of the mCherry-tagged protein, and appropriate negative
309 controls (samples without the GFP-tagged protein) should be included to determine the specificity
310 of the signal.

311 ## Use of IGF in cell extracts from other organisms

312 Although IGF detection is based on endogenous FP fluorescence and thus should not be
313 affected by the cellular context in which these proteins are expressed, we tested the use of this
314 technique in other eukaryotic systems, including Drosophila cells or tissues (**Figure 9, A-B**), MDCK
315 cells (**Figure 9, C**) and *Caenorhabditis elegans* whole organisms (**Figure 9D**). Protein extracts were
316 prepared from FP-expressing cells in native conditions, resuspended in Laemmli buffer and samples
317 were loaded on SDS-PAGE gels (see Material and Methods). Overall, only minor adaptations to
318 current protein extraction protocols were made, and in all cases, IGF was observed, indicating the
319 applicability of IGF detection to the analysis of protein lysates from other organisms. In particular,
320 detection of the EGFP-tagged plasma membrane transducer Smoothened (SMO), which is
321 phosphorylated in response to Hedgehog (Jia et al., 2004) shows that IGF detection can be used to
322 study membrane proteins and post-translational modifications. In the case of total extracts from *C.*
323 *elegans* worms, we could detect GFP and mCherry fluorescence signals, however, we observed the
324 presence of non-specific fluorescent signals in the green channel that may complicate the readout
325 of IGF. First, autofluorescence of *C. elegans* animals was previously reported (Pincus et al., 2016),
326 and using red fluorescent proteins would avoid this problem. Second, we propose additional ways
327 to circumvent this problem. A band migrating just below the 70-kDa marker appeared in lysates from
328 WT animals which did not express any FP construct (**Figure 9D**), but this band disappeared upon
329 denaturation at 50°C. A fluorescent smear of unknown origin was also observed at around 250 kDa
330 (**Supp Fig 9A**), which resisted the denaturation at 50°C. However, this smear was not visible when
331 running the samples on homemade gels compared to commercial, pre-cast gels (**Supp Fig 9B**),
332 probably because this fluorescent material did not migrate into the resolving gel. Whereas these
333 observations provide ways to circumvent the non-specific green fluorescence observed in *C.*
334 *elegans*, it remains that care should be taken when setting up IGF detection in other material,
335 including the use of negative, non-FP-tagged extracts to ensure the specificity of the signal.
336

337 # Discussion

338 Our study introduces in-gel fluorescence (IGF) detection as a rapid and cost-effective
339 alternative to traditional immunoblotting for visualizing fluorescent protein (FPs) signals in cell
340 extracts from yeast and other organisms, with minor adaptations of current protocols. The key points
341 resulting from our observations and optimizations are summarized in **Figure 10.**

342 Our work builds on the widespread use of FPs, particularly green and red fluorescent proteins
343 and their derivatives, as powerful tools in cell biology. GFP, originally developed as a live-cell
344 imaging marker, has since become key for various applications, including the monitoring of protein
345 expression and as a proteomic tool. Immunoblotting has traditionally been the method of choice to
346 visualize and quantify the expression of FP-tagged proteins. However, it comes with drawbacks, as
347 this is a time-consuming experiment with a substantial cost due to the reagents required, and is not
348 optimal for quanatifications compared to fluorescence-based approaches. Here, we propose IGF
349 detection as a fast, easy and efficient alternative to this technique.

350 Our study offers a comprehensive examination of IGF detection as an innovative tool for
351 protein detection after SDS-PAGE. We provide a systematic comparison of a number of widely used
352 FPs. Our evaluation considered key parameters such as fluorescence intensity, heat-stability, and
353 their overall suitability for IGF detection in the context of standard SDS-PAGE protocols and
354 accessible imaging devices. Importantly, this technique can be performed without major adaptation
355 of classical protocols except that protein denaturation should be carried out at low temperatures.

356 Overall, IGF detection is also a cost-effective method. This technique eliminates the need for
357 specific antibodies, which may even not be available in the case of less conventional FPs, as well
358 as nitrocellulose membrane or ECL reagents. This makes it an attractive option for labs that operate
359 under budget constraints. Because the observation is done directly from the gel after migration with
360 no additional steps, problems frequently observed with immunoblotting can be avoided, such as
361 heterogeneity of protein transfer, uneven antibody deposition, stains, and uneven ECL spreading on
362 the membrane.

363 Moreover, IGF is a time-saving technique, bypassing the need for protein transfer and
364 blotting/washing steps, as proteins can be visualized immediately after migration. For example, we
365 were able to use this technique to quickly screen for GFP-containing clones directly on colonies after
366 transformation (See Material and Methods). This complementary approach to PCR-based screening
367 allows to quickly monitor protein expression and size in multiple clones. The advantages of IGF
368 detection are even more appealing in the case of co-immunoprecipitations of two fluorescent
369 proteins, since both the prey and the bait can be visualized within minutes after migration, without
370 interference of primary antibody/secondary antibody recognition which can sometimes hinder signal
371 analysis and quantification.

372 Another key advantage of IGF detection is its versatility. All fluorescent proteins tested gave
373 a fluorescent signal in gels, which is advantageous notably in the case of FPs for which antibodies

are not yet available. However, not all FPs perform equally under all conditions. The results show variations in the efficiency of IGF detection, emphasizing the need to consider both the FP's fluorescence properties and its resistance to denaturation. Our findings demonstrate that EGFP and sfGFP, in particular, display strong in-gel signals and good resistance to denaturation. These features make them prime candidates for IGF applications. Moreover, mCherry stands out for its exceptional heat-stability, maintaining its fluorescence even at relatively high denaturing temperatures. This expands the possibilities of IGF detection to proteins that require higher denaturation temperatures (such as proteins forming dimers or assembled in tight complexes). In all cases, though, the intensity of the signal and the ability to specifically detect a fluorophore depend on the available filters on the imaging systems, which were sometimes limiting (especially in the case of mCherry) and led to bleed-through of signals when visualizing green- and red-tagged proteins in the same sample.

Since fluorescent signals originate from the protein itself, the IGF detection method reduces potential biases that can be encountered after using primary and secondary antibodies. Like all fluorescence detection protocols, signal detection does not depend on a chemiluminescence enzymatic reaction, which imposes kinetic constraints and whose activity can vary depending on substrate accessibility. Depending on the antibody used, and thanks to the constant improvement in the sensitivity of imaging devices, we found that IGF detection could outperform antibody-based chemiluminescent detection, and the signal was globally more linear with respect to protein concentration. Moreover, changing acquisition settings may increase sensitivity, with less background than observed with chemiluminescence.

However, like all techniques, IGF has its limitations. In particular, this technique relies on a partial denaturation of proteins at lower temperatures than usually performed in classical protocols. Depending on the FP used for tagging, proteins treated in mild denaturation conditions can migrate as 2 discrete bands corresponding to the fluorescent and denatured forms of the FP. The apparent molecular weight of FP-tagged proteins is usually lower than under classical denaturation conditions, with up to 15-kDa difference with the denatured form in the case of mRuby2. Furthermore, antibodies may recognize denatured and non-denatured forms of the FPs with different affinities. Although IGF was compatible with a range of lysis buffers, it is also possible that the composition of the lysis buffer in which proteins are resuspended may alter overall fluorescence, depending on the abilities of FPs to remain folded and fluorescent in these conditions. While these factors do not diminish the value of IGF, they highlight the need for appropriate controls when setting up IGF for protein detection.

The method's simplicity, cost-effectiveness, reliability and compatibility with existing FPs and current protocols make IGF detection an attractive alternative to immunoblotting which can greatly benefit research in a range of fields. From basic molecular biology to more applied biomedical research, IGF offers a robust and economical solution to detect fluorescent proteins in gels. Future studies could further explore the method's robustness across different cell types and conditions, ensuring its broad applicability in diverse experimental settings.

412 # Material and Methods

413 ## Yeast strains and cultures.

414 Strains are derivatives of the BY4741 background and are listed in Supplementary Table 1.
415 Proteins were tagged with various FPs at their endogenous loci by homologous recombination using
416 plasmids listed in Supplementary Table 2, or originated from the collection of GFP-tagged strains
417 (Huh et al., 2003). All yeast strains were constructed by transformation with the standard lithium
418 acetate–polyethylene glycol protocol using homologous recombination and verified by polymerase
419 chain reaction (PCR) on genomic DNA. Yeast cells were grown in YPD medium (2% w/v) or in SC
420 medium [containing yeast nitrogen base (1.7 g/L; MP Biomedicals), ammonium sulfate (5 g/liter,
421 Sigma-Aldrich), the appropriate drop-out amino acid preparations (MP Biomedicals), and 2% (w/v)
422 glucose, unless otherwise indicated]. Precultures were incubated at 30°C for 8 hours and diluted in
423 the evening to 20-mL cultures to reach mid-log phase the next morning.

424 ## Preparation of cell lysates from yeast

425 Exponentially growing cells (5 OD_{600} equivalents) were washed twice in water and resuspended
426 in 100µL of cold native lysis buffer [Tris-HCl pH 8.0, 100 mM, NaCl, 0.15 M, Glycerol 5% v/v, Triton
427 X-100 0.5% v/v, PMSF 0.5 mM, Complete antiprotease EDTA free (Roche, #11836170001)], and
428 incubated for 5 min on ice-cold water with glass beads (Sigma-Aldrich, #G8772) to cool samples
429 down prior to lysis. Cells were then lysed in a cold room on a vortex (4 x 30 sec, with 1 min incubation
430 on ice-cold water between each lysis). Cell lysates were retrieved by piercing the bottom of the 1.5-
431 mL tubes and brief centrifugation in a minispin centrifuge. Lysates were cleared by centrifugation at
432 4°C for 5 min at 3,000 xg. Supernatants were collected and 4X Laemmli sample buffer (Bio-Rad,
433 #161-0747) containing DTT (12.5 µM final concentration) was added to the lysates (1X final
434 concentration). Samples were denatured as indicated for each experiment, and loaded on a SDS-
435 PAGE gel.
436 To use IGF from colonies growing on plates for screening purposes, 3 days-old colonies were
437 harvested and resuspended in 100 µL cold native lysis buffer [Tris-HCl pH 8.0, 100 mM, NaCl, 0.15
438 M, Glycerol 5% v/v, Triton X-100 0.5% v/v, PMSF 0.5 mM, Complete antiprotease EDTA free (Roche,
439 #11836170001)] and lysed as described above for exponentially growing cells. 15 µL of lysate were
440 collected and 4X Laemmli sample buffer (Bio-Rad, #161-0747) containing DTT (12.5 µM final
441 concentration) was added to the lysates (1X final concentration). Samples were denatured at 30°C
442 for 5 min, and 20 µL were loaded on SDS-PAGE gel.
443 Relative quantitations were carried out with a detergent-compatible Bradford reagent (Abcam,
444 #ab119216), and samples were then incubated for 5 min. Denaturation temperatures varied from
445 30°C to 95°C and are indicated in the Results section and the Figures. Equivalent protein amounts

446 were loaded on commercial precast 4-20% TGX gels (Bio-Rad, #4561094), and run in Tris-glycine-
447 SDS (TGS) buffer at 150 V for 45 min unless otherwise indicated.

448 Preparation of yeast protein extracts with TCA

449 A volume of culture corresponding to 1 OD_{600} equivalent of exponentially growing yeast cells
450 was collected, to which TCA (100%, w/v; Sigma-Aldrich) was added (10% final concentration).
451 Whole cells were precipitated on ice for 10 min, samples were then centrifuged at 16,000 xg at 4°C
452 for 10 min, the pellet was resuspended in 100 µL of a 10% (w/v) TCA solution and broken for 10 min
453 with glass beads (Sigma-Aldrich, #G8772) at room temperature. Lysates were transferred to another
454 1.5-mL tube to remove glass beads and centrifuged for 5 min at 16,000 xg at 4°C. Protein pellets
455 were resuspended in 50 µL of 1X Laemmli sample buffer, which included 50 mM Tris-base (final
456 concentration) to buffer for the TCA present in the pellet.

457 Preparation of cell lysates from Drosophila cultured cells

458 Drosophila wing imaginal disc cultured cells [Clone 8 (Cl-8) cells] responsive to Hedgehog (HH)
459 were cultured and transiently transfected using transitory insect transfection reagent (Mirusbio, #
460 MIR 6100) using pAct-EGFP, pAct-SMO-EGFP, and pAct-HH (Malpel et al., 2007; Sanial et al.,
461 2017) as described previously (Sanial et al., 2017). Forty-eight hours after transfection, cells were
462 washed in PBS and lysed in 1% Triton X-100, 150 mM NaCl, 50 mM Tris-HCl pH 8.0, 1 mM
463 dithiothreitol with complete EDTA-free antiprotease mix (Roche, #11836170001) and PhosSTOP
464 (Roche, #04906837001). Lysates were centrifuged (12,000 xg) for 10 min at 4°C and the
465 supernatant was mixed with 4X Laemmli sample buffer (Bio-Rad) containing DTT (12.5 µM final
466 concentration). Samples were incubated for 5 minutes at 25°C before loading on a homemade 10%
467 acrylamide gel without SDS. Gels were run for 90 min at 150 V in TGS buffer on a MiniProtean setup
468 (Bio-Rad).

469 Preparation of cell lysates from fly ovary tissue

470 Ovary extracts were obtained from Ptub64c-GAL4 and Ptub64c-GAL4; UbiEGFP-PAR3
471 transgenic flies (Kullmann and Krahn, 2018) by dissecting ovaries (20 flies per genotype) into 1X
472 PBS. Ovaries were placed on ice in lysis buffer [10 mM Tris-HCl pH 7.5, 150 mM NaCl, Complete
473 Protease Inhibitor cocktail (Roche)] and mechanically homogenized using micro pestles in matching
474 tubes. Ovaries lysates were spun at 3000 xg for 20 min at 4°C to eliminate debris. Supernatants
475 were incubated for 5 min at 72°C in LDS sample buffer with Sample Reducing Agent (ThermoFisher,
476 #NP0007). Samples were loaded on a NuPage, 4–12% Bis-Tris gels (ThermoFisher, #NP0322) and
477 run in 1X MOPS buffer (ThermoFisher, #NP0001) for 90 min at 150v.

478 ## Preparation of cell lysates from MDCK cells

479 MDCK cells (ATCC CCL-34) were transfected with Lipofectamine 2000 (Thermofisher
480 #11668027) as described (Walch et al., 2018). Arf1-EGFP and Arf1-mCherry plasmids were
481 obtained by subcloning Arf1 (Wessels et al., 2006) into pEGFP-N3 (Clontech) and pmCherry-N1
482 (Clontech), respectively. Cells were lysed in 6-well plates at confluency with 200 µL of lysis buffer
483 [Tris-HCl pH 8.0 50 mM, NaCl 150mM, EDTA 10 mM, Triton X-100 0.5% (v/v) with complete
484 antiprotease mix (Roche #11836145001)]. After 20 min incubation on ice, cells were scraped from
485 the plate, collected in tubes and vortexed 3 x 5 sec, with 30 sec-incubation on ice between each
486 step. Lysates were cleared by centrifugation 30 min, 11000 xg at 4°C. After protein quantitation using
487 a Bradford reagent (Bio-Rad #5000205), samples were mixed with Laemmli sample buffer (Bio-Rad
488 #161-0747) (1X final concentration). 50 µg of proteins were loaded per well on a precast 4-20%TGX
489 gel (Bio-Rad, #4561094), and run in TGS buffer at 200 V for 45 min.

490 ## Preparation of cell lysates from *C. elegans*

491 Worms [*C. elegans* strain N2 (wildtype ancestral, Bristol) and JDU233: *ijmSi63 [pJD520;*
492 *mosII_5'mex-5_GFP::tba-2; mCherry::his-11; cb-unc-119(+)] II; unc-119(ed3) III* (Lacroix et al.,
493 2024)] were cultured on MGM++ plate and fed on OP50 bacterial strain at 23C. Worm lysate was
494 obtained from an asynchronous population. A total volume equivalent of 50 µL worm pellet was
495 washed twice in bacterial M9 minimal medium containing 0.05% (v/v) Tween-20, resuspended into
496 200 µL Lysis buffer [50mM Tris-HCl pH 8.0, 200 mM NaCl, 5% glycerol and Complete protease
497 inhibitor cocktail (Roche #11836145001)] and sonicated for 1 min on ice. Total extract was incubated
498 for 5 min at 50°C with 1x final pH8 Laemmli sample buffer containing DTT (12.5 µM final
499 concentration). 40 µg of worm extract were loaded per well onto a precast 4-20%TGX gel (Bio-Rad,
500 #4561094), and run in TGS buffer at 200 V for 45 min.

501 ## In-gel fluorescence imaging

502 After migration, the gel was imaged with gel-imaging systems whose excitation/emission
503 wavelengths were compatible with the observation of green and red fluorescent proteins. Imaging
504 with the Amersham Typhoon 5 (Cytiva) was carried out using the 488 nm laser with the Cy2 filter
505 525BP20 (for green FPs) or the 532 nm laser with the Cy3 filter LPG550 (for red FPs). The scanning
506 resolution was 25 µm/pixel. PMT voltage was adjusted so that collected signals do not saturate.
507 Imaging on the Chemidoc MP (Bio-Rad) was carried out using standard excitation/emission
508 wavelengths recommended for Cy2/Cy3 filters (green FP: Epi-blue, excitation: 460−490 nm,
509 emission: 518–546 nm; red FP: Epi-green, excitation: 520−545 nm, emission: 577–613 nm).
510 Total proteins were visualized by in-gel fluorescence using a trihalo compound incorporated in
511 the commercial pre-cast SDS–PAGE gels (stain-free TGX gels, 4–20%; Bio-Rad) after 45 sec UV-

512 induced photoactivation using a ChemiDoc MP imager (Bio-Rad), serving as a loading control. Note
513 that UV irradiation should preferentially be performed after FP imaging (see **Figure S2**).

514 Immunoblotting

515 After fluorescence imaging, gels were equilibrated in transfer buffer [25 mM Tris, 190 mM
516 glycine, 20% ethanol (v/v), 0.02% SDS (w/v)] for 15 min and transferred at 100 V onto a nitrocellulose
517 membrane in a liquid transfer system (MiniProtean, Bio-Rad). Membranes were blocked in Tris-
518 buffered saline solution (50 mM Tris pH 7.6, 150 mM NaCl) containing 0.1 % Tween-20 (v/v) (TBS-
519 T) and 2% fat-free milk (w/v) for 30 min and incubated for at least 2 hours with the appropriate
520 primary antibodies. Membranes were washed 3 x 10 min in TBS-T and incubated for at least two
521 hours with the corresponding secondary antibody (coupled with horseradish peroxidase or
522 Alexa680). Membranes were then washed again 3 x 10 min in TBS-T and incubated with ECL Select
523 Western Blotting Detection Reagent (Cytiva #RPN2235) except in **Figure S3B** in which Clarity
524 Western ECL Substrate (Bio-Rad #1705060) was used because of the strong signal obtained with
525 the anti-GFP antibody 3H9. Luminescence signals were acquired using a ChemiDoc MP (Bio-Rad).
526 For denaturation of proteins on the membrane (**Figure S3B**), the membrane treatment was adapted
527 from Xu et al (2019) (Xu et al., 2019): after transfer, the membrane was washed with water, incubated
528 with cold 50% methanol (v/v) on ice for 30 min. The membrane was then washed with water, quickly
529 dried on lint-free wipes and incubated in a sandwich between two sheets of Whatman paper and two
530 glass slides at 75°C in a preheated thermocycler for 30 min.

531 Antibodies

532 The primary antibodies used are: anti-GFP (clones 7.1 and 13.1; Roche #11814460001; 1/5,000
533 dilution), Anti-GFP (Chromotek #3H9; 1/5,000), anti-GFP-DyLight800 (Rockland, #600-145-215;
534 1/2,000), anti-Bmh1 (kind gift of S. Lemmon, Univ. Miami, USA; 1/15,000) (Gelperin et al., 1995);
535 anti-Hkx2 (Rockland, #100-4159; 1/3,000). Secondary antibodies are anti-Mouse IgG-HRP (Sigma-
536 Aldrich, #A5278; 1/5000), anti-Rabbit IgG-HRP (Sigma-Aldrich, #A6154; 1/5,000), anti-Rat IgG-HRP
537 (Jackson Immuno, #112-035-143; 1/5,000), and anti-Mouse IgG Alexa Fluor 680 (ThermoFisher,
538 #21057; 1/5,000).

539 Test of the linearity of the signal by sample dilution

540 Extraction was performed in native conditions using 15 OD_{600} equivalent of yeast lysed in 300
541 µL of cold native lysis buffer [100 mM Tris-HCl pH 8.0, NaCl 0.15 M, Glycerol 5% v/v, Triton X-100
542 0.5% v/v, PMSF 0.5 mM, Complete antiprotease EDTA free (Roche, #11836170001)]. 4X Laemmli
543 sample buffer (Biorad) was added to the lysates (1X final, 12.5 µM DTT final concentration), and
544 samples were then incubated for 5 min at 30°C. Samples were serial-diluted with 1X native sample
545 buffer (62.5 mM Tris-HCl pH 6.8, 10% glycerol (v/v), 0.005% bromophenol blue (w/v)], as follows: 9

546 times at 0.75X dilution, followed by 5 times at 0.5X dilution (final dilution >300 fold). Fluorescence
547 levels were quantified using ImageQuant TL v8.2 (Cytiva).

548 Sample denaturation with a range of temperatures

549 Extraction was performed in native conditions using 15OD_{600} equivalent of yeast lysed in 300µL
550 of cold native lysis buffer [100 mM Tris-HCl pH 8.0, NaCl 0.15 M, Glycerol 5% v/v, Triton X-100 0.5%
551 v/v, PMSF 0.5 mM, Complete antiprotease EDTA free (Roche, #11836170001)]. 4X Laemmli sample
552 buffer was added to the lysates (1X final, DTT 12.5 µM final concentration). Samples were distributed
553 in 0.5 mL Eppendorf tube and kept on ice until heat treatment. Samples were heated at various
554 temperatures in an Eppendorf Gradient Mastercycler for 5 min, and kept at 22°C after incubation.
555 The equivalent of 0.5 OD_{600} was loaded in each well. Fluorescence levels were quantified using
556 ImageQuant TL v8.2 (Cytiva).

557 Co-immunoprecipitations of fluorescent proteins from yeast lysates

558 Exponentially growing cells (40 OD_{600} equivalents) were washed twice in water and
559 resuspended in 400 µL of cold IP lysis buffer (100 mM Tris-HCl pH8, NaCl 200 mM, Glycerol 5%,
560 Triton X-100 0.1%, EDTA 1 mM) containing protease inhibitors [PMSF 0.5 mM, Complete
561 antiprotease EDTA free (Roche, #11836170001), NaF 10 mM], and incubated for 5 min on ice-cold
562 water with glass beads. Cells were then lysed in a cold room on a vortex (4 x 30 sec, with 1 min
563 incubation on ice-cold water between each lysis). Relative quantitation was made with Bradford
564 reagent to use equivalent amounts of proteins for co-immunoprecipitation. Samples were diluted
565 4:10 as per the manufacturer's instructions with dilution buffer (10 mM Tris-HCl pH 8.0, NaCl 200
566 mM, EDTA 1 mM) containing protease inhibitors [PMSF 0.5 mM, Complete antiprotease EDTA free
567 (Roche, #11836170001), NaF 10 mM]. A fraction (3%) was taken as the "Input" fraction. 10 µL GFP-
568 Trap Magnetic Particles M-270 (Proteintech, #gtd) or RFP-Trap Magnetic Agarose (Proteintech,
569 #rtma) were added to the remaining of the sample and incubated on a rotating wheel for 1h at 4°C
570 and washed 3 times with cold IP lysis buffer. Proteins were eluted in 40 µL of FP trap sample buffer
571 [66 mM Tris-HCl pH 8.0, 2% SDS, 100 mM NaCl, 12.5 µM DTT, 10% (v/v) glycerol, 0.002%
572 bromophenol blue (w/v)] by incubating at 50°C for 20 min with soft shaking in a dry bath incubator.
573 Half of the IP and 1% of the diluted lysate were loaded on the gel.

574 ### Construction of yeast-optimized mCherry and mNeonGreen

575 The mCherry and mNeonGreen sequences were codon-optimized for *Saccharomyces*
576 *cerevisiae* using GENEius tool (giving ymCherry and ymNeonGreen, respectively) and synthetized
577 (Eurofins Genomics), with a GSAGAGAGAGAG or GSGAGAGAGAGAGA linker respectively,
578 flanked by the traditional S1/S3 oligo sequences used for amplification (Janke et al., 2004). Linkers
579 were also codon-optimized but sequences are different to avoid recombination. DNA was provided
580 cloned into pEX-A128 containing a polylinker site to allow subcloning into the pYM vector series
581 (Janke et al., 2004) with various selection markers. ymNeonGreen was cloned in pYM16 at
582 BsiW1/AscI sites, giving pYM-ymCherry-NAT (pSL778), and ymCherry was cloned in pYM17 at
583 HindIII/AscI sites, giving pYM-ymNeonGreen-Hph (pSL766).

584 ## Acknowledgments

585 The authors wish to thank Dr Silke Hauf (Virginia Tech, Blacksburg, VA, USA), Dr Sandra
586 Lemmon (University of Miami, Coral Gables, FL, USA), Dr Myriam Ruault (Institut Curie, Paris,
587 France), Dr Julien Dumont (Institut Jacques Monod, Paris, FR) and Dr Alenka Copic (CRBM,
588 Montpellier, FR) for sharing material, and Dr Catherine L. Jackson (Institut Jacques Monod, Paris,
589 FR) for discussions and critical reading of the manuscript. This work was supported by grants from
590 Université Paris-Cité IDEx (https://u-paris.fr; ANR-18-IDEX-0001, "Emergence en Recherche"
591 RS30J20IDXA1_EMERLEON) and Agence Nationale pour la Recherche ("AMPKILL", ANR-23-
592 CE13-0012-01) to S. Léon. N. Joly is supported by a grant from the Fondation ARC pour la recherche
593 sur le cancer (ARCPJA2022050005002) and a grant from Université Paris-Cité IDEx (https://u-
594 paris.fr; ANR-18-IDEX-0001, "Emergence en Recherche" RS30J23IDX64_KATAREP).
595 The authors declare no competing interests.
596
597

598 # References

599 Bird, L.E., H. Rada, A. Verma, R. Gasper, J. Birch, M. Jennions, J. Löwe, I. Moraes, and R.J. Owens.
600 2015. Green fluorescent protein-based expression screening of membrane proteins in
601 Escherichia coli. *J Vis Exp*:e52357.
602 Bomholt, J., C. Helix-Nielsen, P. Scharff-Poulsen, and P.A. Pedersen. 2013. Recombinant
603 production of human Aquaporin-1 to an exceptional high membrane density in
604 Saccharomyces cerevisiae. *PLoS One*. 8:e56431.
605 Brachmann, C.B., A. Davies, G.J. Cost, E. Caputo, J. Li, P. Hieter, and J.D. Boeke. 1998. Designer
606 deletion strains derived from Saccharomyces cerevisiae S288C: a useful set of strains and
607 plasmids for PCR-mediated gene disruption and other applications. *Yeast*. 14:115-132.
608 Campbell, R.E., O. Tour, A.E. Palmer, P.A. Steinbach, G.S. Baird, D.A. Zacharias, and R.Y. Tsien.
609 2002. A monomeric red fluorescent protein. *Proc Natl Acad Sci U S A*. 99:7877-7882.
610 Chalfie, M., Y. Tu, G. Euskirchen, W.W. Ward, and D.C. Prasher. 1994. Green fluorescent protein
611 as a marker for gene expression. *Science*. 263:802-805.
612 Chandris, P., C.C. Giannouli, and G. Panayotou. 2021. Imaging Approaches for the Study of
613 Metabolism in Real Time Using Genetically Encoded Reporters. *Front Cell Dev Biol*.
614 9:725114.
615 Chaudhri, M., M. Scarabel, and A. Aitken. 2003. Mammalian and yeast 14-3-3 isoforms form distinct
616 patterns of dimers in vivo. *Biochemical and Biophysical Research Communications*. 300:679-
617 685.
618 Chew, F.N., W.S. Tan, T.C. Ling, C.S. Tan, and B.T. Tey. 2009. Quantitation of green fluorescent
619 protein using a gel-based imaging method. *Anal Biochem*. 384:353-355.
620 Cormack, B.P., G. Bertram, M. Egerton, N.A.R. Gow, S. Falkow, and A.J.P. Brown. 1997. Yeast-
621 enhanced green fluorescent protein (yEGFP): a reporter of gene expression in Candida
622 albicans. *Microbiology (Reading)*. 143 (Pt 2):303-311.
623 Cormack, B.P., R.H. Valdivia, and S. Falkow. 1996. FACS-optimized mutants of the green
624 fluorescent protein (GFP). *Gene*. 173:33-38.
625 Cristea, I.M., R. Williams, B.T. Chait, and M.P. Rout. 2005. Fluorescent proteins as proteomic
626 probes. *Mol Cell Proteomics*. 4:1933-1941.
627 Donate-Macian, P., E. Alvarez-Marimon, F. Sepulcre, J.L. Vazquez-Ibar, and A. Peralvarez-Marin.
628 2019. The Membrane Proximal Domain of TRPV1 and TRPV2 Channels Mediates Protein(-
629)Protein Interactions and Lipid Binding In Vitro. *Int J Mol Sci*. 20.
630 Eaton, S.L., M.L. Hurtado, K.J. Oldknow, L.C. Graham, T.W. Marchant, T.H. Gillingwater, C.
631 Farquharson, and T.M. Wishart. 2014. A guide to modern quantitative fluorescent western
632 blotting with troubleshooting strategies. *J Vis Exp*:e52099.
633 Geertsma, E.R., M. Groeneveld, D.J. Slotboom, and B. Poolman. 2008. Quality control of
634 overexpressed membrane proteins. *Proc Natl Acad Sci U S A*. 105:5722-5727.
635 Gelperin, D., J. Weigle, K. Nelson, P. Roseboom, K. Irie, K. Matsumoto, and S. Lemmon. 1995. 14-
636 3-3 proteins: potential roles in vesicular transport and Ras signaling in *Saccharomyces*
637 *cerevisiae*. *Proc Natl Acad Sci U S A*. 92:11539-11543.
638 Hochreiter, B., A.P. Garcia, and J.A. Schmid. 2015. Fluorescent proteins as genetically encoded
639 FRET biosensors in life sciences. *Sensors (Basel)*. 15:26281-26314.
640 Hu, C.D., and T.K. Kerppola. 2003. Simultaneous visualization of multiple protein interactions in
641 living cells using multicolor fluorescence complementation analysis. *Nat Biotechnol*. 21:539-
642 545.
643 Huh, W.K., J.V. Falvo, L.C. Gerke, A.S. Carroll, R.W. Howson, J.S. Weissman, and E.K. O'Shea.
644 2003. Global analysis of protein localization in budding yeast. *Nature*. 425:686-691.
645 Janke, C., M.M. Magiera, N. Rathfelder, C. Taxis, S. Reber, H. Maekawa, A. Moreno-Borchart, G.
646 Doenges, E. Schwob, E. Schiebel, and M. Knop. 2004. A versatile toolbox for PCR-based
647 tagging of yeast genes: new fluorescent proteins, more markers and promoter substitution
648 cassettes. *Yeast*. 21:947-962.
649 Jia, J., C. Tong, B. Wang, L. Luo, and J. Jiang. 2004. Hedgehog signalling activity of Smoothened
650 requires phosphorylation by protein kinase A and casein kinase I. *Nature*. 432:1045-1050.
651 Khmelinskii, A., P.J. Keller, A. Bartosik, M. Meurer, J.D. Barry, B.R. Mardin, A. Kaufmann, S.
652 Trautmann, M. Wachsmuth, G. Pereira, W. Huber, E. Schiebel, and M. Knop. 2012. Tandem

fluorescent protein timers for in vivo analysis of protein dynamics. *Nat Biotechnol*. 30:708-714.

Krasnoselska, G.O., M. Dumoux, N. Gamage, H. Cheruvara, J. Birch, A. Quigley, and R.J. Owens. 2021. Transient Transfection and Expression of Eukaryotic Membrane Proteins in Expi293F Cells and Their Screening on a Small Scale: Application for Structural Studies. *Methods Mol Biol*. 2305:105-128.

Kullmann, L., and M.P. Krahn. 2018. Redundant regulation of localization and protein stability of DmPar3. *Cell Mol Life Sci*. 75:3269-3282.

Lacroix, B., S. Vigneron, J.C. Labbe, L. Pintard, C. Lionne, G. Labesse, A. Castro, and T. Lorca. 2024. Increases in cyclin A/Cdk activity and in PP2A-B55 inhibition by FAM122A are key mitosis-inducing events. *EMBO J*. 43:993-1014.

Lam, A.J., F. St-Pierre, Y. Gong, J.D. Marshall, P.J. Cranfill, M.A. Baird, M.R. McKeown, J. Wiedenmann, M.W. Davidson, M.J. Schnitzer, R.Y. Tsien, and M.Z. Lin. 2012. Improving FRET dynamic range with bright green and red fluorescent proteins. *Nat Methods*. 9:1005-1012.

Lambert, T.J. 2019. FPbase: a community-editable fluorescent protein database. *Nat Methods*. 16:277-278.

Lee, S., W.A. Lim, and K.S. Thorn. 2013. Improved blue, green, and red fluorescent protein tagging vectors for S. cerevisiae. *PLoS One*. 8:e67902.

Leon, S., Z. Erpapazoglou, and R. Haguenauer-Tsapis. 2008. Ear1p and Ssh4p are new adaptors of the ubiquitin ligase Rsp5p for cargo ubiquitylation and sorting at multivesicular bodies. *Mol Biol Cell*. 19:2379-2388.

Longtine, M.S., A. McKenzie, 3rd, D.J. Demarini, N.G. Shah, A. Wach, A. Brachat, P. Philippsen, and J.R. Pringle. 1998. Additional modules for versatile and economical PCR-based gene deletion and modification in Saccharomyces cerevisiae. *Yeast*. 14:953-961.

Madani, G., E. Lamping, H.J. Lee, M. Niimi, A.K. Mitra, and R.D. Cannon. 2021. Small-Scale Plasma Membrane Preparation for the Analysis of Candida albicans Cdr1-mGFPHis. *J Vis Exp*.

Malpel, S., S. Claret, M. Sanial, A. Brigui, T. Piolot, L. Daviet, S. Martin-Lanneree, and A. Plessis. 2007. The last 59 amino acids of Smoothened cytoplasmic tail directly bind the protein kinase Fused and negatively regulate the Hedgehog pathway. *Dev Biol*. 303:121-133.

Merzlyak, E.M., J. Goedhart, D. Shcherbo, M.E. Bulina, A.S. Shcheglov, A.F. Fradkov, A. Gaintzeva, K.A. Lukyanov, S. Lukyanov, T.W. Gadella, and D.M. Chudakov. 2007. Bright monomeric red fluorescent protein with an extended fluorescence lifetime. *Nat Methods*. 4:555-557.

Muller-Lucks, A., S. Bock, B. Wu, and E. Beitz. 2012. Fluorescent in situ folding control for rapid optimization of cell-free membrane protein synthesis. *PLoS One*. 7:e42186.

Nakatani, T., N. Yasui, I. Tamura, and A. Yamashita. 2019. Specific modification at the C-terminal lysine residue of the green fluorescent protein variant, GFPuv, expressed in Escherichia coli. *Scientific reports*. 9:4722.

Nemec, A.A., L.A. Howell, A.K. Peterson, M.A. Murray, and R.J. Tomko, Jr. 2017. Autophagic clearance of proteasomes in yeast requires the conserved sorting nexin Snx4. *J Biol Chem*. 292:21466-21480.

Newstead, S., H. Kim, G. von Heijne, S. Iwata, and D. Drew. 2007. High-throughput fluorescent-based optimization of eukaryotic membrane protein overexpression and purification in Saccharomyces cerevisiae. *Proc Natl Acad Sci U S A*. 104:13936-13941.

Pedelacq, J.D., S. Cabantous, T. Tran, T.C. Terwilliger, and G.S. Waldo. 2006. Engineering and characterization of a superfolder green fluorescent protein. *Nat Biotechnol*. 24:79-88.

Pincus, Z., T.C. Mazer, and F.J. Slack. 2016. Autofluorescence as a measure of senescence in C. elegans: look to red, not blue or green. *Aging (Albany NY)*. 8:889-898.

Romei, M.G., and S.G. Boxer. 2019. Split Green Fluorescent Proteins: Scope, Limitations, and Outlook. *Annu Rev Biophys*. 48:19-44.

Rothbauer, U., K. Zolghadr, S. Muyldermans, A. Schepers, M.C. Cardoso, and H. Leonhardt. 2008. A versatile nanotrap for biochemical and functional studies with fluorescent fusion proteins. *Mol Cell Proteomics*. 7:282-289.

Rothbauer, U., K. Zolghadr, S. Tillib, D. Nowak, L. Schermelleh, A. Gahl, N. Backmann, K. Conrath, S. Muyldermans, M.C. Cardoso, and H. Leonhardt. 2006. Targeting and tracing antigens in live cells with fluorescent nanobodies. *Nat Methods*. 3:887-889.

Ruan, Z., J. Lee, Y. Li, J. Du, and W. Lu. 2023. Human Pannexin 1 Channel is NOT Phosphorylated by Src Tyrosine Kinase at Tyr199 and Tyr309. *bioRxiv*.

Saeed, I.A., and S.S. Ashraf. 2009. Denaturation studies reveal significant differences between GFP and blue fluorescent protein. *Int J Biol Macromol*. 45:236-241.

Sanial, M., I. Becam, L. Hofmann, J. Behague, C. Arguelles, V. Gourhand, L. Bruzzone, R.A. Holmgren, and A. Plessis. 2017. Dose-dependent transduction of Hedgehog relies on phosphorylation-based feedback between the G-protein-coupled receptor Smoothened and the kinase Fused. *Development*. 144:1841-1850.

Shaner, N.C., R.E. Campbell, P.A. Steinbach, B.N. Giepmans, A.E. Palmer, and R.Y. Tsien. 2004. Improved monomeric red, orange and yellow fluorescent proteins derived from Discosoma sp. red fluorescent protein. *Nat Biotechnol*. 22:1567-1572.

Shaner, N.C., G.G. Lambert, A. Chammas, Y. Ni, P.J. Cranfill, M.A. Baird, B.R. Sell, J.R. Allen, R.N. Day, M. Israelsson, M.W. Davidson, and J. Wang. 2013. A bright monomeric green fluorescent protein derived from Branchiostoma lanceolatum. *Nat Methods*. 10:407-409.

Shaner, N.C., M.Z. Lin, M.R. McKeown, P.A. Steinbach, K.L. Hazelwood, M.W. Davidson, and R.Y. Tsien. 2008. Improving the photostability of bright monomeric orange and red fluorescent proteins. *Nat Methods*. 5:545-551.

Shaner, N.C., P.A. Steinbach, and R.Y. Tsien. 2005. A guide to choosing fluorescent proteins. *Nat Methods*. 2:905-909.

Subach, F.V., O.M. Subach, I.S. Gundorov, K.S. Morozova, K.D. Piatkevich, A.M. Cuervo, and V.V. Verkhusha. 2009. Monomeric fluorescent timers that change color from blue to red report on cellular trafficking. *Nat Chem Biol*. 5:118-126.

Terskikh, A., A. Fradkov, G. Ermakova, A. Zaraisky, P. Tan, A.V. Kajava, X. Zhao, S. Lukyanov, M. Matz, S. Kim, I. Weissman, and P. Siebert. 2000. "Fluorescent timer": protein that changes color with time. *Science*. 290:1585-1588.

Tsien, R.Y. 1998. The green fluorescent protein. *Annu Rev Biochem*. 67:509-544.

Wach, A., A. Brachat, C. Alberti-Segui, C. Rebischung, and P. Philippsen. 1997. Heterologous HIS3 marker and GFP reporter modules for PCR-targeting in Saccharomyces cerevisiae. *Yeast*. 13:1065-1075.

Walch, L., E. Pellier, W. Leng, G. Lakisic, A. Gautreau, V. Contremoulins, J.M. Verbavatz, and C.L. Jackson. 2018. GBF1 and Arf1 interact with Miro and regulate mitochondrial positioning within cells. *Scientific reports*. 8:17121.

Wang, M., Y. Da, and Y. Tian. 2023. Fluorescent proteins and genetically encoded biosensors. *Chem Soc Rev*. 52:1189-1214.

Ward, W.W. 2005. Biochemical and Physical Properties of Green Fluorescent Protein. *In* Green Fluorescent Protein. 39-65.

Weinberger Ii, J., and C.W. Lennon. 2021. Monitoring Protein Splicing Using In-gel Fluorescence Immediately Following SDS-PAGE. *Bio Protoc*. 11:e4121.

Wessels, E., D. Duijsings, T.K. Niu, S. Neumann, V.M. Oorschot, F. de Lange, K.H. Lanke, J. Klumperman, A. Henke, C.L. Jackson, W.J. Melchers, and F.J. van Kuppeveld. 2006. A viral protein that blocks Arf1-mediated COP-I assembly by inhibiting the guanine nucleotide exchange factor GBF1. *Dev Cell*. 11:191-201.

White, J., and E. Stelzer. 1999. Photobleaching GFP reveals protein dynamics inside live cells. *Trends Cell Biol*. 9:61-65.

Wosika, V., E. Durandau, C. Varidel, D. Aymoz, M. Schmitt, and S. Pelet. 2016. New families of single integration vectors and gene tagging plasmids for genetic manipulations in budding yeast. *Mol Genet Genomics*. 291:2231-2240.

Xu, J., H. Sun, G. Huang, G. Liu, Z. Li, H. Yang, L. Jin, X. Cui, L. Shi, T. Ma, A. Kameyama, and W. Dong. 2019. A fixation method for the optimisation of western blotting. *Scientific reports*. 9:6649.

Xu, Q., and T.A. Keiderling. 2004. Effect of sodium dodecyl sulfate on folding and thermal stability of acid-denatured cytochrome c: a spectroscopic approach. *Protein Sci*. 13:2949-2959.

Zacharias, D.A., J.D. Violin, A.C. Newton, and R.Y. Tsien. 2002. Partitioning of lipid-modified monomeric GFPs into membrane microdomains of live cells. *Science*. 296:913-916.

765 # Figure legends

766 Figure 1. Detection of in-gel fluorescence from endogenously expressed proteins
767 tagged with yeGFP.

768 A. Control (WT) yeast or yeast expressing Bmh1-yeGFP, Hxk1-yeGFP were lysed in the
769 indicated conditions (Nat.: native conditions; TCA: lysis in denaturing conditions with TCA),
770 samples were resuspended in LDS sample buffer (1X final, Bio-Rad) and incubated for 5 min
771 at the indicated temperatures. After migration on a commercial precast 4-20% TGX gels (Bio-
772 Rad), gels were imaged for green fluorescence using a Typhoon and a Chemidoc MP, and
773 total proteins were visualized by the stain-free technology on a Chemidoc MP. After transfer
774 to a nitrocellulose membrane, proteins were immunoblotted with anti-GFP antibodies
775 (Roche) and detected by chemiluminescence using anti-mouse antibodies coupled to HRP.
776 B. Protein lysates were prepared as in A. Proteins were incubated at 30°C or 95°C for 5 min,
777 with and without prior incubation at 30°C (5 min). After migration on a commercial precast 4-
778 20%TGX gel (Bio-Rad), gels were imaged for green fluorescence using a Chemidoc MP, and
779 total proteins were visualized by the stain-free technology on a Chemidoc MP. Proteins were
780 then transferred to a nitrocellulose membrane and imaged again for yeGFP fluorescence,
781 which was maintained during transfer. Proteins were then immunoblotted with anti-GFP
782 antibodies (Roche) and anti-mouse antibodies coupled to Alexa Fluor 680. yeGFP
783 fluorescence was then visualized again before detecting the anti-GFP antibodies by
784 fluorescence on a Chemidoc MP.

785 Figure 2. Comparison of in-gel fluorescence of yeGFP-, GFP(S65T)- and EGFP-tagged
786 proteins

787 A. Yeast expressing Bmh1-yeGFP, Bmh1-GFP(S65T), Hxk1-yeGFP and Hxk1-GFP(S65T)
788 were lysed in native conditions, samples were resuspended in LDS sample buffer and
789 incubated for 5 min at the indicated temperatures. After migration on a commercial precast
790 4-20% TGX gels (Bio-Rad), gels were imaged for green fluorescence using a Chemidoc MP,
791 and total proteins were visualized by the stain-free technology on a Chemidoc MP. Proteins
792 were then transferred to a nitrocellulose membrane and imaged again for green
793 fluorescence, which was maintained during transfer. Proteins were then immunoblotted with
794 anti-GFP antibodies (Roche) and anti-mouse antibodies coupled to Alexa Fluor 680. Green
795 fluorescence was then visualized again before detecting the anti-GFP antibodies by
796 fluorescence. The membranes were then stripped and incubated with anti-Bmh1 or anti-
797 Hxk1/2 antibodies and then with anti-rabbit antibodies coupled to HRP, and revealed by
798 chemiluminescence on a Chemidoc MP.

799 B. Yeast expressing Bmh1-yeGFP and Bmh1-EGFP were lysed in native conditions, samples
800 were resuspended in LDS sample buffer and incubated for 5 min at the indicated
801 temperatures. After migration on a commercial precast 4-20% TGX gel (Bio-Rad), gels were
802 imaged for green fluorescence using a Typhoon or a Chemidoc MP, and total proteins were
803 visualized by the stain-free technology on a Chemidoc MP. Proteins were then transferred to
804 a nitrocellulose membrane and immunoblotted with anti-Bmh1 antibodies and then with anti-
805 rabbit antibodies coupled to HRP, and revealed by chemiluminescence on a Chemidoc MP.
806 * indicates the fluorescent species.

807 Figure 3. Comparison of in-gel fluorescence of yeGFP-, sfGFP- and mNeonGreen-
808 tagged proteins

809 Yeast expressing Bmh1-yeGFP, Bmh1-sfGFP or Bmh1-mNeonGreen were lysed in native
810 conditions, samples were resuspended in LDS sample buffer and incubated for 5 min at the
811 indicated temperatures. After migration on a commercial precast 4-20%TGX gel (Bio-Rad), gels
812 were imaged for green fluorescence using a Typhoon or a Chemidoc MP, and total proteins were
813 visualized by the stain-free technology on a Chemidoc MP. Proteins were then transferred to a
814 nitrocellulose membrane and immunoblotted with anti-Bmh1 antibodies and then with anti-rabbit
815 antibodies coupled to HRP, and revealed by chemiluminescence on a Chemidoc MP. * indicates
816 the fluorescent species.

817 Figure 4. Temperature-sensitivity of in-gel fluorescence of yeGFP-, EGFP- and sfGFP-
818 tagged proteins

819 A. Yeast expressing Bmh1-yeGFP were lysed in native conditions, samples were resuspended
820 in LDS sample buffer and incubated for 5 min at the indicated temperatures in a gradient
821 thermocycler (note that the temperature range is different for sfGFP). After migration on a
822 commercial precast 4-20%TGX gel (Bio-Rad), gels were imaged for green fluorescence
823 using a Typhoon, and total proteins were visualized by the stain-free technology on a
824 Chemidoc MP. Proteins were then transferred to a nitrocellulose membrane and
825 immunoblotted with anti-Bmh1 antibodies and then with anti-rabbit antibodies coupled to
826 HRP, and revealed by chemiluminescence on a Chemidoc MP.
827 B. Same as A. using yeast expressing Bmh1-EGFP.
828 C. Same as A. using yeast expressing Bmh1-sfGFP.
829 D. Quantification of the green fluorescence signal as a function of the denaturation temperature
830 for various green FP-tagged Bmh1 (n=3; ± SD). Solid line: sigmoidal fit of the data (GraphPad
831 Prism), dotted line: 95% confidence interval of the fit.

832 Figure 5. Comparison of in-gel fluorescence of tagRFP-T-, mRuby2- and mCherry-
833 tagged proteins

834 A. Yeast expressing Bmh1-tagRFP-T, Bmh1-mRuby2 or Bmh1-mCherry were lysed in native
835 conditions, samples were resuspended in LDS sample buffer and incubated for 5 min at the
836 indicated temperatures. After migration on a commercial precast 4-20%TGX gel (Bio-Rad),
837 gels were imaged for red fluorescence using a Typhoon or a Chemidoc MP, and total proteins
838 were visualized by the stain-free technology on a Chemidoc MP. Proteins were then
839 transferred to a nitrocellulose membrane and immunoblotted with anti-Bmh1 antibodies and
840 then with anti-rabbit antibodies coupled to HRP, and revealed by chemiluminescence on a
841 Chemidoc MP. * indicates the fluorescent species.
842 B. Yeast expressing Bmh1-mCherry were lysed in native conditions, samples were
843 resuspended in LDS sample buffer and incubated for 5 min at the indicated temperatures in
844 a gradient thermocycler. After migration on a commercial precast 4-20%TGX gel (Bio-Rad),
845 gels were imaged for red fluorescence using a Typhoon, and total proteins were visualized
846 by the stain-free technology on a Chemidoc. Proteins were then transferred to a nitrocellulose
847 membrane and immunoblotted with anti-Bmh1 antibodies and then with anti-rabbit antibodies
848 coupled to HRP, and revealed by chemiluminescence on a Chemidoc MP.
849 C. Quantification of the red fluorescence signal as a function of the denaturation temperature
850 for mCherry-tagged Bmh1 (n=3; ±SD). Solid line: sigmoidal fit of the data (GraphPad Prism),
851 dotted line: 95% confidence interval of the fit.

852 Figure 6. Sensitivity and linearity of in-gel fluorescence detection of EGFP

853 A. *Left.* Yeast expressing Bmh1-EGFP were lysed in native conditions, samples were
854 resuspended in LDS sample buffer and incubated for 5 min at 30°C. Samples were serially
855 diluted (right to left) into sample buffer without LDS (see Material and Methods), and loaded
856 onto on a commercial precast 4-20%TGX gel (Bio-Rad). After migration, gels were imaged
857 for green fluorescence using a Typhoon, and proteins were then transferred to a
858 nitrocellulose membrane and immunoblotted with anti-Bmh1 antibodies and then with anti-
859 rabbit antibodies coupled to HRP, and revealed by chemiluminescence on a Chemidoc MP.
860 *Right.* Quantification of the signals obtained for green fluorescence (black) and
861 chemiluminescence (red) as a function of sample dilution. Linear-scaled and log-plot scaled
862 graphs are shown.
863 B. *Left.* Same experiment as in A, but using anti-GFP antibodies and anti-mouse antibodies
864 coupled to HRP to reveal proteins by chemiluminescence. *Right.* Quantification of the signals
865 obtained for fluorescence (black) and chemiluminescence (red) as a function of sample
866 dilution. Linear-scaled and log-plot scaled graphs are shown.

867 Figure 7. High pH preserves green fluorescence in diluted protein samples

868 A. Design of the experiment. Protein lysates prepared in native conditions from yeast
869 expressing Bmh1-EGFP are diluted 1:5 with dilution buffer (water, lysis buffer, NaCl at
870 various concentrations, or 100 mM Tris-HCl solution at various pH) before mixing with 4X
871 sample buffer pH6.8 (1X final concentration). Samples are then incubated at 50°C for 10 min
872 before being loaded on SDS-PAGE.
873 B. Effect of lysis buffer and NaCl concentration on in-gel fluorescence. Samples were diluted
874 with water, native lysis buffer (1X, 0.75X, 0.5X or 0.25X in water) or NaCl solution (at the
875 indicated concentration) before being incubated at 50°C for 10 min. After migration on a
876 commercial precast 4-20%TGX gel (Bio-Rad), gels were imaged for green fluorescence
877 using a Typhoon, and total proteins were visualized by the stain-free technology on a
878 Chemidoc MP. Proteins were then transferred to a nitrocellulose membrane and
879 immunoblotted with anti-GFP antibodies and then with anti-mouse antibodies coupled to
880 HRP, and revealed by chemiluminescence on a Chemidoc MP.
881 C. Effect of pH on in-gel fluorescence. Samples were diluted with native lysis buffer (1X), water
882 or Tris-HCl 100 mM solution (final concentration) at the indicated pH before being incubated
883 at 50°C for 10 min. After migration on a commercial precast 4-20%TGX gel (Bio-Rad), gels
884 were imaged for green fluorescence using a Typhoon, and total proteins were visualized by
885 the stain-free technology on a Chemidoc MP.

886 Figure 8. IGF detection in the context of co-immunoprecipitation

887 A. Protein lysates prepared in native conditions with native IP lysis buffer from yeast expressing
888 Bmh2-ymCherry (a yeast codon-optimized mCherry) with or without the co-expression of
889 Bmh1-yeGFP were subjected to co-immunoprecipitation using GFP-trap beads.
890 Immunoprecipitates were incubated at 50°C for 20 min in 1X Laemmli sample buffer at pH
891 8.0 which allows to maintain protein fluorescence at low protein concentrations. Input
892 samples and immunoprecipitates (IP) are shown. After migration on a commercial precast 4-
893 20%TGX gel (Bio-Rad), gels were imaged for green and red fluorescence using a Typhoon,
894 and total proteins were visualized by the stain-free technology on a Chemidoc MP. * indicates
895 bleed-through of the green fluorescence into the red channel.
896 B. Protein lysates prepared in native conditions from yeast expressing Bmh1-yeGFP with or
897 without the co-expression of Bmh2-ymCh were subjected to co-immunoprecipitation using
898 RFP-trap beads and treated as in A. Input samples and immunoprecipitates (IP) are shown.
899 After migration on a commercial precast 4-20%TGX gel (Bio-Rad), gels were imaged for
900 green and red fluorescence using a Typhoon, and total proteins were visualized by the stain-
901 free technology on a Chemidoc MP.

902 Figure 9. IGF detection in cells from various organisms

903 A. Drosophila wing-imaginal-disc cultured cells [Clone 8 (Cl-8) cells] were transfected with
904 plasmids encoding the Hedgehog (HH) transducer Smoothened (SMO) fused to EGFP and
905 EGFP alone. They were also transfected (+) or not (-) with a construct allowing the
906 expression of HH. Cells were lysed in native conditions (see Material and Methods), lysates
907 were mixed with 4X Laemmli sample buffer and incubated for 5 minutes at 25°C before
908 loading on a homemade PAGE gel. IGF was detected on a Typhoon. SMO-EGFP is
909 phosphorylated in the presence of HH, causing a slower migration (red arrowhead).
910 B. Transgenic *Drosophila* flies expressing or not an EGFP-tagged version of the polarity protein
911 PAR-3 were dissected and ovaries were lysed in native conditions (see Material and
912 Methods). Samples were incubated for 5 min at 72°C in LDS sample buffer, loaded on a
913 NuPage Bis-Tris gel (ThermoFisher) and IGF was detected on a Typhoon after migration.
914 After fluorescence imaging, total proteins were stained with Coomassie stain and imaged on
915 the infrared channel on a Chemidoc MP.
916 C. MDCK cells expressing Arf1 fused to EGFP or mCherry were lysed in native conditions (see
917 Material and Methods). Samples were incubated for 10 min at 50°C in LDS sample buffer
918 and loaded on a gel. After migration on a commercial precast 4-20%TGX gel (Bio-Rad), gels
919 were imaged for green and red fluorescence using a Chemidoc MP, and total proteins were
920 visualized by the stain-free technology on a Chemidoc MP. Note that some bleed-through of
921 green fluorescence is observed in the red channel (see also **Fig. 8A** and **Fig. S8**).
922 D. Transgenic *C. elegans* expressing or not GFP-tagged alpha-tubulin and mCherry-tagged
923 histone H2B were lysed in native conditions (see Material and Methods) by sonication.
924 Samples were incubated for 5 min at 50°C in Laemmli sample buffer (pH 8.0). After migration
925 on a commercial precast 4-20%TGX gel (Bio-Rad), gels were imaged for green and red
926 fluorescence using a Typhoon, and total proteins were visualized by the stain-free technology
927 on a Chemidoc MP. * denotes a non-specific fluorescence protein present in extracts of WT
928 *C. elegans* whose fluorescence disappears when heating the sample at 50°C.

929 Figure 10. Overview of the workflow and technical considerations when using IGF
930 detection to visualize proteins in gel.

931 White boxes refer to figure panels in which specific points are addressed.
932

933

934 # Supplementary material

935 ## Supplementary tables.

936 **Table S1: Yeast strains used in this study**

Name	Genotype & Description	Origin & Reference
ySL0066: **BY4741 (WT)**	*MAT a; ura3Δ0, his3Δ1, leu2Δ0, met15Δ0*	(Brachmann et al., 1998)
ySL2719: **Bmh1-yeGFP**	*MAT a; ura3Δ0, his3Δ1, leu2Δ0, met15Δ0; BMH1-yeGFP::KANMX*	This study
ySL3509: **Hxk1-yeGFP**	*MAT a; ura3Δ0, his3Δ1, leu2Δ0, met15Δ0; HXK1-yeGFP::HPHNT1*	This study
ySL0435: **Bmh1-GFP(S65T)**	*MAT a; ura3Δ0, his3Δ1, leu2Δ0, met15Δ0; BMH1:GFP(S65T)::HIS3MX6*	(Huh et al., 2003)
ySL3674: **Bmh1-EGFP**	*MAT a; ura3Δ0, his3Δ1, leu2Δ0, met15Δ0; BMH1-EGFP::HIS3MX6*	This study
ySL3422: **Bmh1-sfGFP**	*MAT a; ura3Δ0, his3Δ1, leu2Δ0, met15Δ0; BMH1-sfGFP::HIS3MX6*	This study
ySL3423: **Bmh1-mNeongreen**	*MAT a; ura3Δ0, his3Δ1, leu2Δ0, met15Δ0; BMH1-mNeonGreen::HPHNT1*	This study
ySL3595: **Bmh1-ymNeongreen**	*MAT a; ura3Δ0, his3Δ1, leu2Δ0, met15Δ0; BMH1-ymNeonGreen::HPHNT1*	This study
ySL3421: **Bmh1-TagRFP-T**	*MAT a; ura3Δ0, his3Δ1, leu2Δ0, met15Δ0; BMH1-TagRFP-T::CaURA3*	This study
ySL3420: **Bmh1-mRuby2**	*MAT a; ura3Δ0, his3Δ1, leu2Δ0, met15Δ0; BMH1-mRUBY2::HIS3MX6*	This study
ySL3419: **Bmh1-mCherry**	*MAT a; ura3Δ0, his3Δ1, leu2Δ0, met15Δ0; BMH1-mCherry::KANMX4*	This study
ySL3593: **Bmh2-ymCherry**	*MAT a; ura3Δ0, his3Δ1, leu2Δ0, met15Δ0; BMH2-ymCherry::NATNT2*	This study
ySL3595: **Bmh2-ymCherry Bmh1-yeGFP**	*MAT a; ura3Δ0, his3Δ1, leu2Δ0, met15Δ0; BMH1-GFP::KanMx4; BMH2-ymCherry::NATNT2*	This study

937

938

939 **Table S2: Plasmids for yeast tagging used in this study**

940

Name	Description	Origin & Reference
pYM12	Plasmid to tag genes with yeGFP at their endogenous locus (*KANMX4*)	(Janke et al., 2004)
pYM25	Plasmid to tag genes with EGFP at their endogenous locus (*HPHNT1*)	(Janke et al., 2004)
pYM28	Plasmid to tag genes with EGFP at their endogenous locus (*HIS3MX6*)	(Janke et al., 2004)
GTH-g (pSL648)	Plasmid to tag genes with sfGFP at their endogenous locus (*HIS3MX6*)	Addgene #81104 (Wosika et al., 2016)
pFA6-mNeongreen::Hph (pSL643)	Plasmid to tag genes with mNeonGreen at their endogenous locus (*HPHNT1*)	Silke Hauf's lab, Virginia Tech
pFa6-link-yoTag-RFP-T-CaURA3 (pSL558)	Plasmid to tag genes with yeast codon-optimized Tag-RFP-T at their endogenous locus (*CaURA3*)	Addgene #44877 (Lee et al., 2013)
pFA6a-link-yomRuby2-SpHIS5 (pS649)	Plasmid to tag genes with yeast codon-optimized Tag-RFP-T at their endogenous locus (*SpHIS5*)	Addgene #44843 (Lee et al., 2013)
pYM-mCherry (pSL1)	Plasmid to tag genes with mCherry at their endogenous locus (*KANMX4*)	(Leon et al., 2008)
pYM-ymCherry-NAT (pSL778)	Plasmid to tag genes with yeast codon-optimized mCherry (*NATNT2*)	This study
pYM-ymNeonGreen-Hph (pSL766)	Plasmid to tag genes with yeast codon-optimized mNeonGreen (*HPHNT1*)	This study

941

942

943 # Supplementary Figure legends.

944 Supplementary Figure 1. Spectral properties of green fluorescent proteins used in this
945 study.

946 A. Excitation wavelengths of yeGFP (= GFPmut3), EGFP, sfGFP and mNeonGreen. Data were
947 retrieved from FPBase (Lambert, 2019). The window of excitation provided by the Chemidoc
948 MP imaging system is indicated in gray (460-490nm), the wavelength of the excitation laser
949 of the Typhoon is indicated as a dotted line (488 nm), as per the manufacturer's indications.
950 B. Emission wavelengths of yeGFP (=GFPmut3), EGFP, sfGFP, and mNeonGreen. Data were
951 retrieved from FPBase (Lambert, 2019) and have been divided by the quantum yield to
952 evaluate fluorescence efficiency for each FP. The window of emission collected by the
953 Chemidoc MP system is indicated in gray (518-546 nm), that of the Typhoon is indicated as
954 shaded (515-535 nm), as per the manufacturer's indications.

955 Supplementary Figure 2. Effect of UV irradiation and freezing on the fluorescence of
956 various fluorescent proteins.

957 A. Native lysates of cells expressing Bmh1 tagged with yeGFP, EGFP, sfGFP, mNeonGreen or
958 mCherry were kept on ice or frozen (-20°C, -80°C, or in liquid N_2) for one hour, thawed on
959 ice and incubated at 30°C for 5 min, and loaded onto SDS-PAGE. IGF was detected on a
960 Chemidoc MP before (top) and after (bottom) UV irradiation, which is required for the
961 "StainFree" labeling (Bio-Rad) of total proteins with a trihalo compound (see Material and
962 Methods).
963 B. Quantification of the effect of UV exposure on IGF (ratio of signal obtained after UV exposure
964 to that obtained before UV exposure, for each fluorophore; n=4; ± SD).

965 Supplementary Figure 3. Effect of denaturation temperature on the recognition of GFP-
966 tagged proteins by various anti-GFP antibodies.

967 A. A native lysate of cells expressing Bmh1-yeGFP was resuspended in LDS sample buffer and
968 incubated at the indicated temperatures. After migration, gels were imaged for green
969 fluorescence using a Chemidoc MP, and total proteins were visualized by the stain-free
970 technology on a Chemidoc MP. Proteins were then transferred to a nitrocellulose membrane,
971 immunoblotted with the indicated antibodies and revealed by chemiluminescence on a
972 Chemidoc MP. * indicates the fluorescent species.
973 B. A native lysate of cells expressing Bmh1-yeGFP was resuspended in LDS sample buffer and
974 incubated at the indicated temperatures. After migration, gels were imaged for green
975 fluorescence using a Chemidoc MP, and total proteins were visualized by the stain-free
976 technology on a Chemidoc MP. Proteins were then transferred to a nitrocellulose membrane

977 and immunoblotted with the indicated antibodies and revealed by chemiluminescence on a
978 Chemidoc MP. Membranes on the right were treated with methanol and high temperature
979 (see Material and Methods) to denature proteins and ameliorate the detection of GFP-tagged
980 proteins treated at low temperatures. * indicates the fluorescent species.

981 Supplementary Figure 4. Comparison of IGF signals of mNeonGreen and a
982 corresponding yeast-optimized version.

983 Yeast expressing Bmh1-mNG and Bmh1-ymNG were lysed in native conditions, samples
984 were resuspended in LDS sample buffer and incubated for 5 min at the indicated temperatures. After
985 migration, gels were imaged for green fluorescence using a Typhoon or a Chemidoc MP, and total
986 proteins were visualized by the stain-free technology on a Chemidoc MP. Proteins were then
987 transferred to a nitrocellulose membrane and immunoblotted with anti-Bmh1 antibodies and then
988 with anti-rabbit antibodies coupled to HRP, and revealed by chemiluminescence on a Chemidoc MP.
989 The size difference is due to a longer linker present in the ymNeonGreen construct.* indicates the
990 fluorescent species.

991 Supplementary Figure 5. Spectral properties of red fluorescent proteins used in this
992 study.

993 A. Excitation wavelengths of mCherry, TagRFP-T and mRuby2. Data were retrieved from
994 FPBase (Lambert, 2019). The window of excitation provided by the Chemidoc MP imaging
995 system is indicated in gray (520-545nm), the wavelength of the excitation laser of the
996 Typhoon is indicated as a dotted line (532 nm), as per the manufacturer's indications.
997 B. Emission wavelengths of mCherry, TagRFP-T and mRuby2. Data were retrieved from
998 FPBase (Lambert, 2019). The window of emission collected by the Chemidoc MP system is
999 indicated in gray (577-613nm), that of the Typhoon is indicated as shaded (≥550 nm), as per
1000 the manufacturer's indications.

1001 Supplementary Figure 6. Effect of sample dilution on FP denaturation.

1002 *Top*, Yeast expressing Bmh1-yeGFP were lysed in native conditions, samples were
1003 resuspended in LDS sample buffer, incubated for 5 min at 30°C and serially diluted (1:2) in LDS
1004 sample buffer. After migration, gels were imaged for green fluorescence using a Typhoon. Proteins
1005 were then transferred to a nitrocellulose membrane and immunoblotted with anti-Bmh1 antibodies
1006 and then with anti-rabbit antibodies coupled to HRP, and revealed by chemiluminescence on a
1007 Chemidoc MP. Red arrowhead: size of the native (fluorescent) protein; blue arrowhead, size of the
1008 denatured protein.
1009 *Bottom*, Quantification of the signals obtained for fluorescence (black) and chemiluminescence
1010 (red: native protein, blue: denatured protein) as a function of sample dilution. Linear-scaled and log-

1011 plot scaled graphs are shown. yeGFP denaturation increases with sample dilution, causing a bias
1012 when quantifying fluorescence.

1013 Supplementary Figure 7. Sensitivity and linearity of in-gel fluorescence detection of
1014 various FP

1015 A. Yeast expressing Bmh1-yeGFP were lysed in native conditions, samples were resuspended
1016 in LDS sample buffer and incubated for 5 min at 30°C. Samples were serially diluted (right
1017 to left) into sample buffer without LDS (see Material and Methods), and loaded onto SDS-
1018 PAGE. After migration, gels were imaged for green fluorescence using a Typhoon, and
1019 proteins were then transferred to a nitrocellulose membrane and immunoblotted with anti-
1020 Bmh1 antibodies and then with anti-rabbit antibodies coupled to HRP, and revealed by
1021 chemiluminescence on a Chemidoc MP. *Right.* Quantification of the signals obtained for
1022 green fluorescence (black) and chemiluminescence (red) as a function of sample dilution.
1023 Linear-scaled and log-plot scaled graphs are shown.
1024 B. Same as A, with Bmh1-sfGFP.
1025 C. Same as A, with Bmh1-mNeonGreen.
1026 D. Same as A, with Bmh1-mCherry.
1027

1028 Supplementary Figure 8. Bleedthrough of green fluorescence in the red fluorescence
1029 channel when using a Chemidoc MP.

1030 The same gel as that presented in **Fig 8A** was imaged for red fluorescence in a Chemidoc MP.
1031 * indicates the green fluorescent signal that is detected in the red channel.
1032

1033 Supplementary Figure 9. Endogenous fluorescent material in *C. elegans* worm extracts.

1034 A. Extended version of the gel presented in **Figure 9D**. Total protein extracts of *C. elegans*
1035 worms were prepared as detailed in *Material and Methods* and loaded onto precast TGX 4-
1036 20% gels (Bio-Rad). After migration, gels were imaged for fluorescence using a Typhoon
1037 at the indicated excitation/emission wavelengths. A fluorescent smear of unknown origin is
1038 visible in the green channel at around 250 kDa.
1039 B. The same samples as in A were loaded onto a precast TGX 4-20% gel (Bio-Rad) (left) or
1040 homemade 10% SDS-PAGE gel (right). After migration, gels were imaged for fluorescence
1041 using a Typhoon at the indicated excitation/emission wavelengths. The fluorescent smear
1042 in the green channel at around 250 kDa was no longer observed in homemade gels.
1043
1044
1045

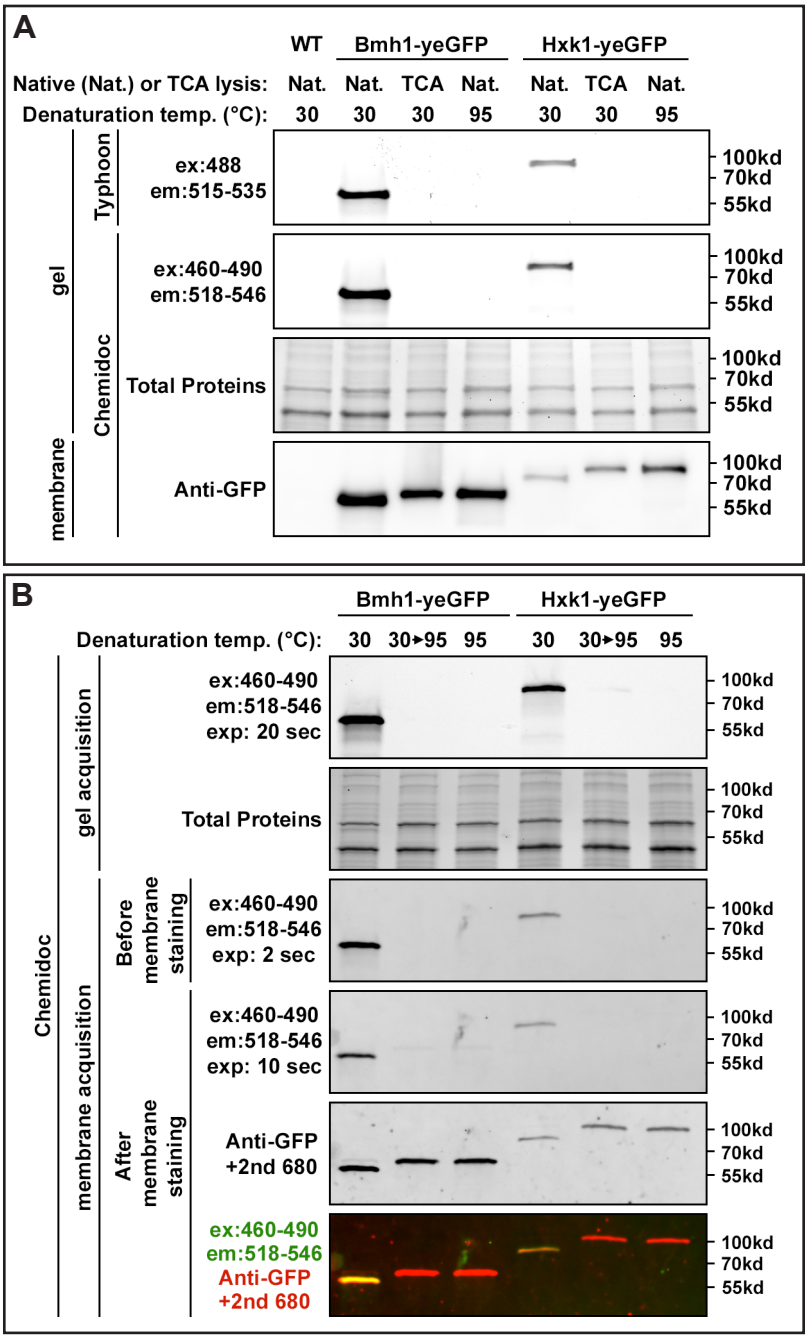
A
WT
Bmh1-yeGFP
Hxk1-yeGFP
Native (Nat.) or TCA lysis:
Nat. Nat. TCA Nat. Nat. TCA Nat.
Denaturation temp. (°C):
30 30 30 95 30 30 95
gel
membrane
Typhoon
Chemidoc
ex:488
em:515-535
ex:460-490
em:518-546
Total Proteins
Anti-GFP
100kd
70kd
55kd
B
Bmh1-yeGFP
Hxk1-yeGFP
Denaturation temp. (°C):
30 30▸95 95 30 30▸95 95
Chemidoc
gel acquisition
membrane acquisition
Before membrane staining
After membrane staining
ex:460-490
em:518-546
exp: 20 sec
Total Proteins
ex:460-490
em:518-546
exp: 2 sec
ex:460-490
em:518-546
exp: 10 sec
Anti-GFP
+2nd 680
ex:460-490
em:518-546
Anti-GFP
+2nd 680
100kd
70kd
55kd

Figure 1

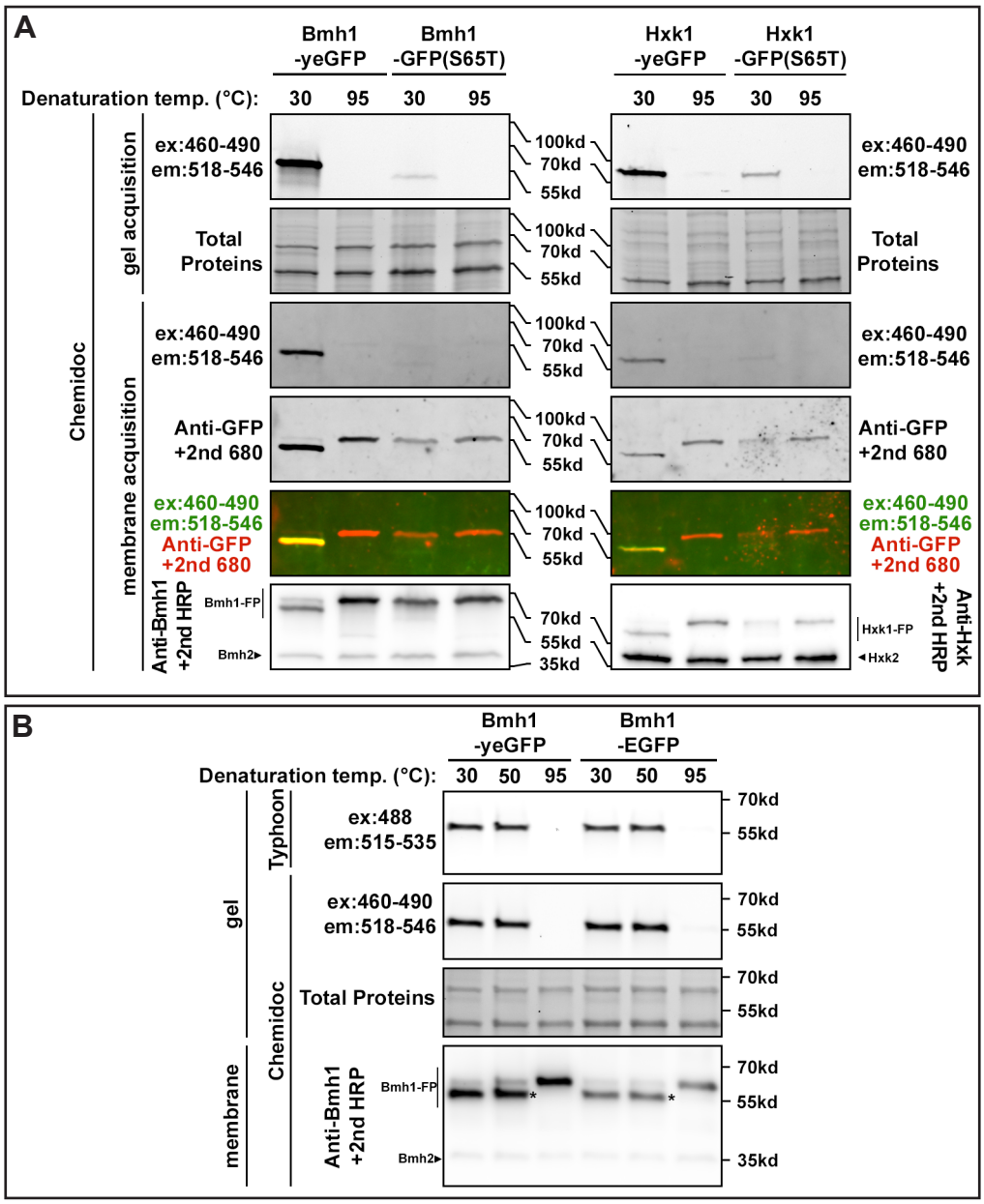
A
Bmh1 -yeGFP
Bmh1 -GFP(S65T)
Hxk1 -yeGFP
Hxk1 -GFP(S65T)
Denaturation temp. (°C):
30 95 30 95
30 95 30 95
Chemidoc
gel acquisition
membrane acquisition
ex:460-490 em:518-546
Total Proteins
Anti-GFP +2nd 680
ex:460-490 em:518-546 Anti-GFP +2nd 680
Anti-Bmh1 +2nd HRP
Anti-Hxk +2nd HRP
Bmh1-FP
Bmh2
Hxk1-FP
Hxk2
100kd
70kd
55kd
35kd
B
Bmh1 -yeGFP
Bmh1 -EGFP
Denaturation temp. (°C):
30 50 95 30 50 95
Typhoon
Chemidoc
gel
membrane
ex:488 em:515-535
ex:460-490 em:518-546
Total Proteins
Anti-Bmh1 +2nd HRP
Bmh1-FP
Bmh2
70kd
55kd
35kd

Figure 2

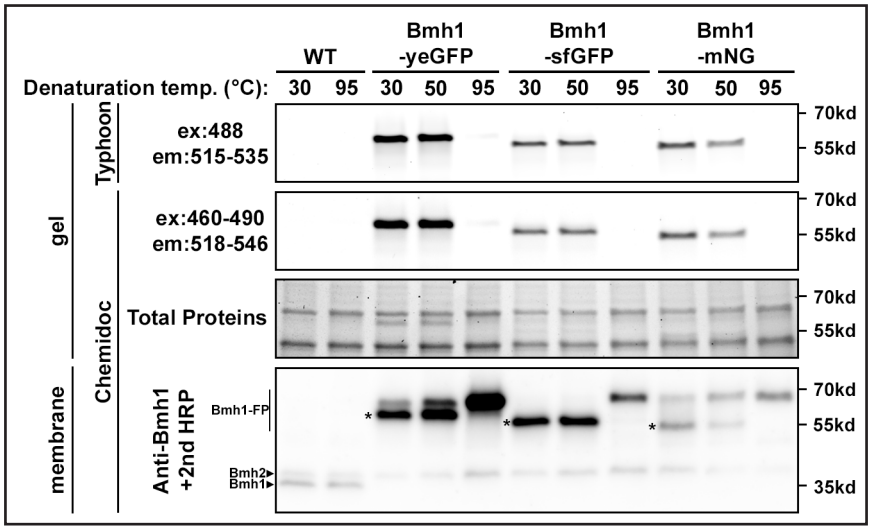
WT
Bmh1 -yeGFP
Bmh1 -sfGFP
Bmh1 -mNG
Denaturation temp. (°C): 30 95 30 50 95 30 50 95 30 50 95
gel
membrane
Typhoon
Chemidoc
ex:488 em:515-535
ex:460-490 em:518-546
Total Proteins
Anti-Bmh1 +2nd HRP
Bmh1-FP
Bmh2
Bmh1
70kd
55kd
35kd

Figure 3

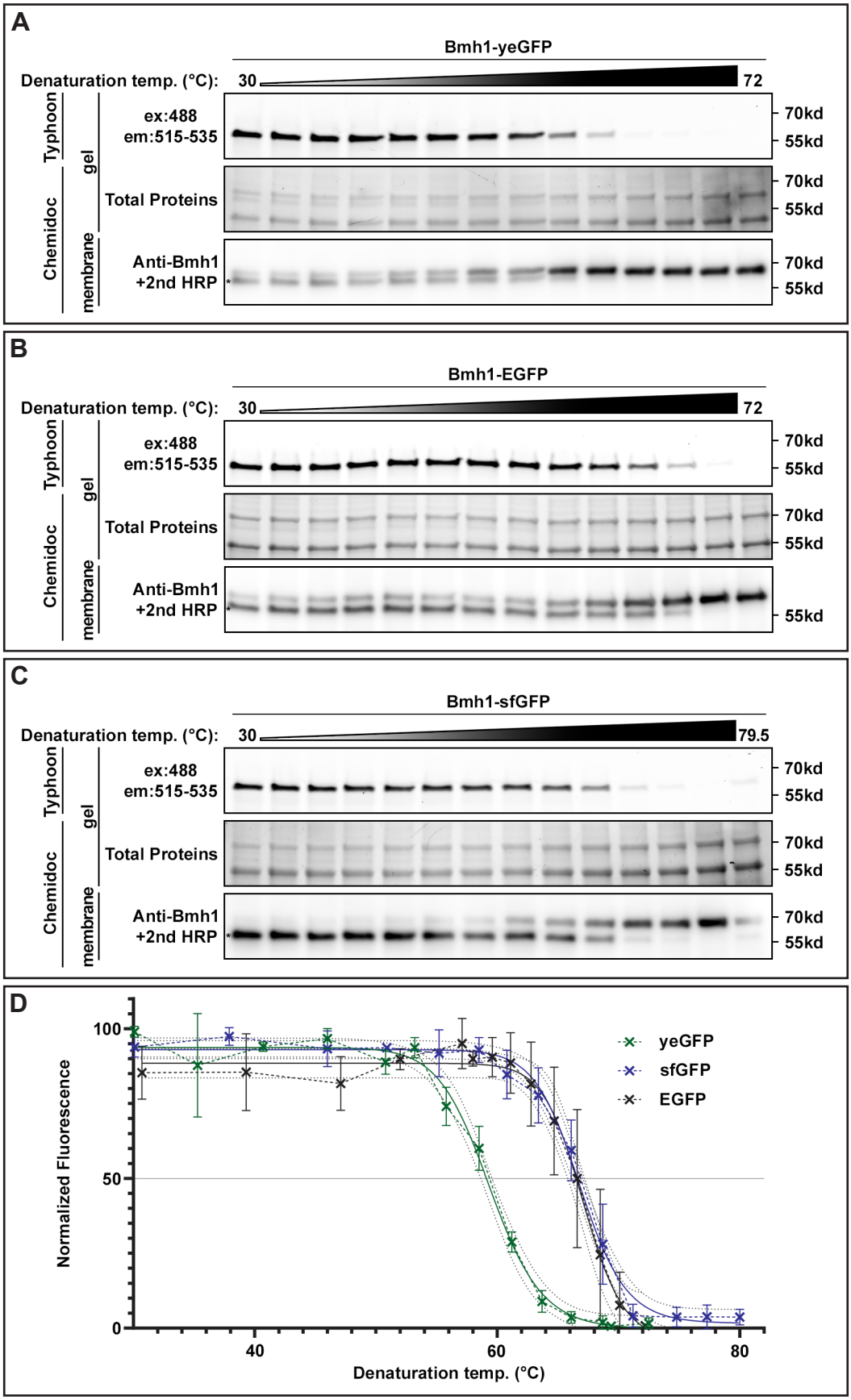
A
Bmh1-yeGFP
Denaturation temp. (°C):
30
72
Typhoon
Chemidoc
gel
membrane
ex:488
em:515-535
Total Proteins
Anti-Bmh1
+2nd HRP
70kd
55kd
B
Bmh1-EGFP
C
Bmh1-sfGFP
79.5
D
Normalized Fluorescence
Denaturation temp. (°C)
yeGFP
sfGFP
EGFP
100
50
0
40
60
80

Figure 4

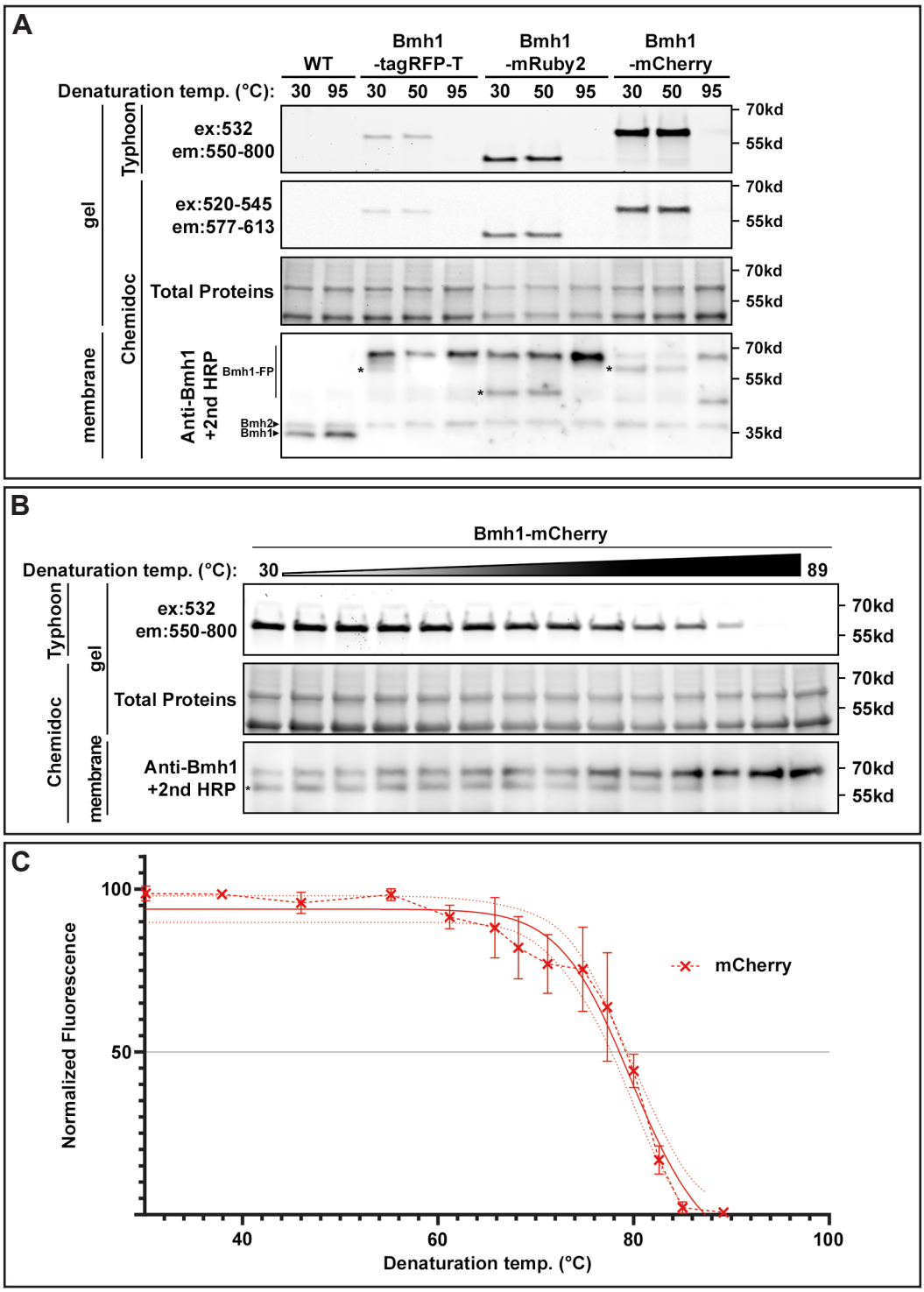
A
WT
Bmh1 -tagRFP-T
Bmh1 -mRuby2
Bmh1 -mCherry
Denaturation temp. (°C): 30 95 30 50 95 30 50 95 30 50 95
gel
membrane
Typhoon
Chemidoc
ex:532 em:550-800
ex:520-545 em:577-613
Total Proteins
Anti-Bmh1 +2nd HRP
Bmh1-FP
Bmh2
Bmh1
70kd
55kd
35kd
B
Bmh1-mCherry
Denaturation temp. (°C): 30 89
Typhoon
Chemidoc
gel
membrane
ex:532 em:550-800
Total Proteins
Anti-Bmh1 +2nd HRP
70kd
55kd
C
Normalized Fluorescence
100
50
40
60
80
100
Denaturation temp. (°C)
mCherry

Figure 5

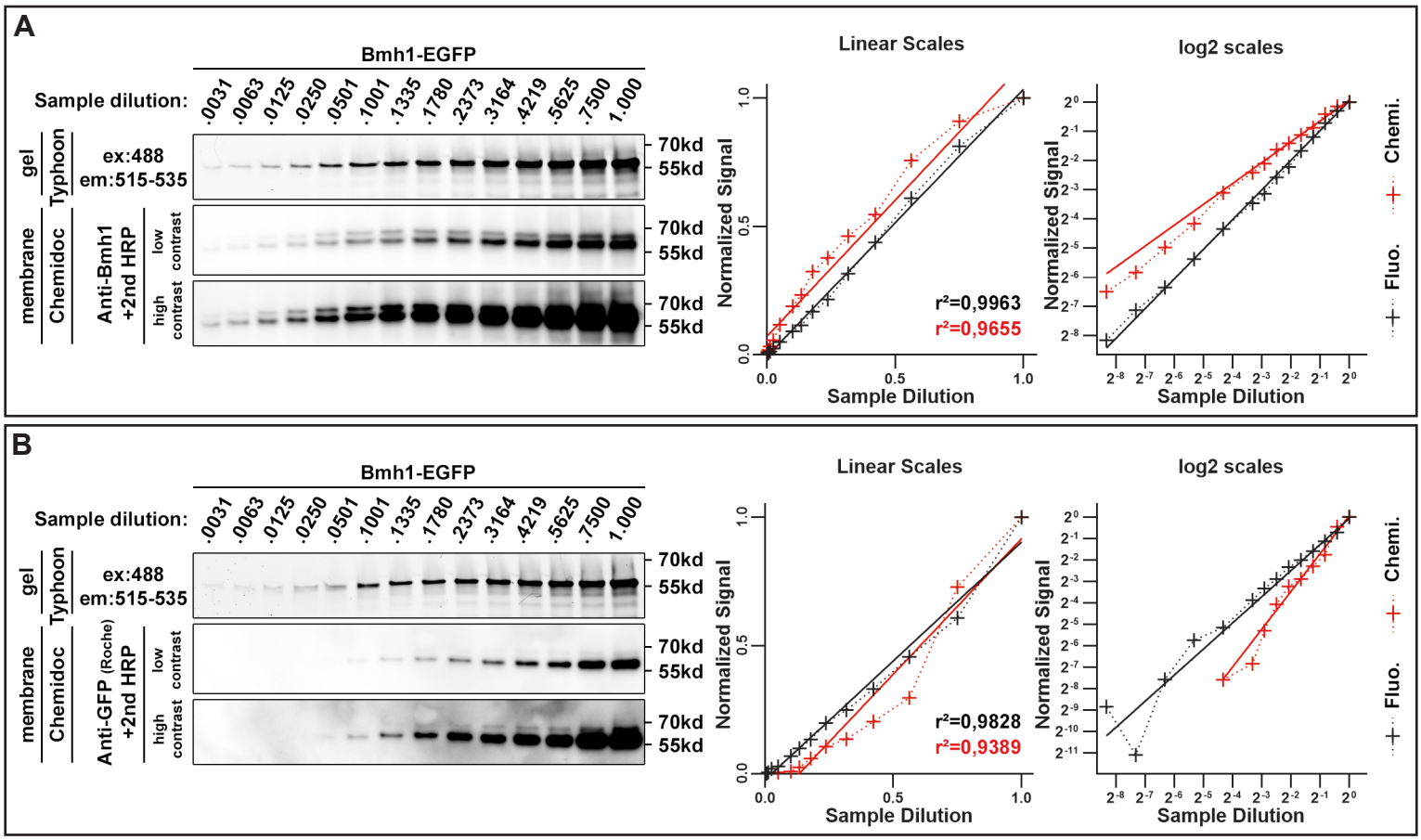
A
Bmh1-EGFP
Sample dilution:
.0031
.0063
.0125
.0250
.0501
.1001
.1335
.1780
.2373
.3164
.4219
.5625
.7500
1.000
gel
Typhoon
ex:488
em:515-535
membrane
Chemidoc
Anti-Bmh1
+2nd HRP
low contrast
high contrast
70kd
55kd
Linear Scales
log2 scales
Normalized Signal
Sample Dilution
r²=0,9963
r²=0,9655
Chemi.
Fluo.

B
Bmh1-EGFP
Sample dilution:
.0031
.0063
.0125
.0250
.0501
.1001
.1335
.1780
.2373
.3164
.4219
.5625
.7500
1.000
gel
Typhoon
ex:488
em:515-535
membrane
Chemidoc
Anti-GFP (Roche)
+2nd HRP
low contrast
high contrast
70kd
55kd
Linear Scales
log2 scales
Normalized Signal
Sample Dilution
r²=0,9828
r²=0,9389
Chemi.
Fluo.

Figure 6

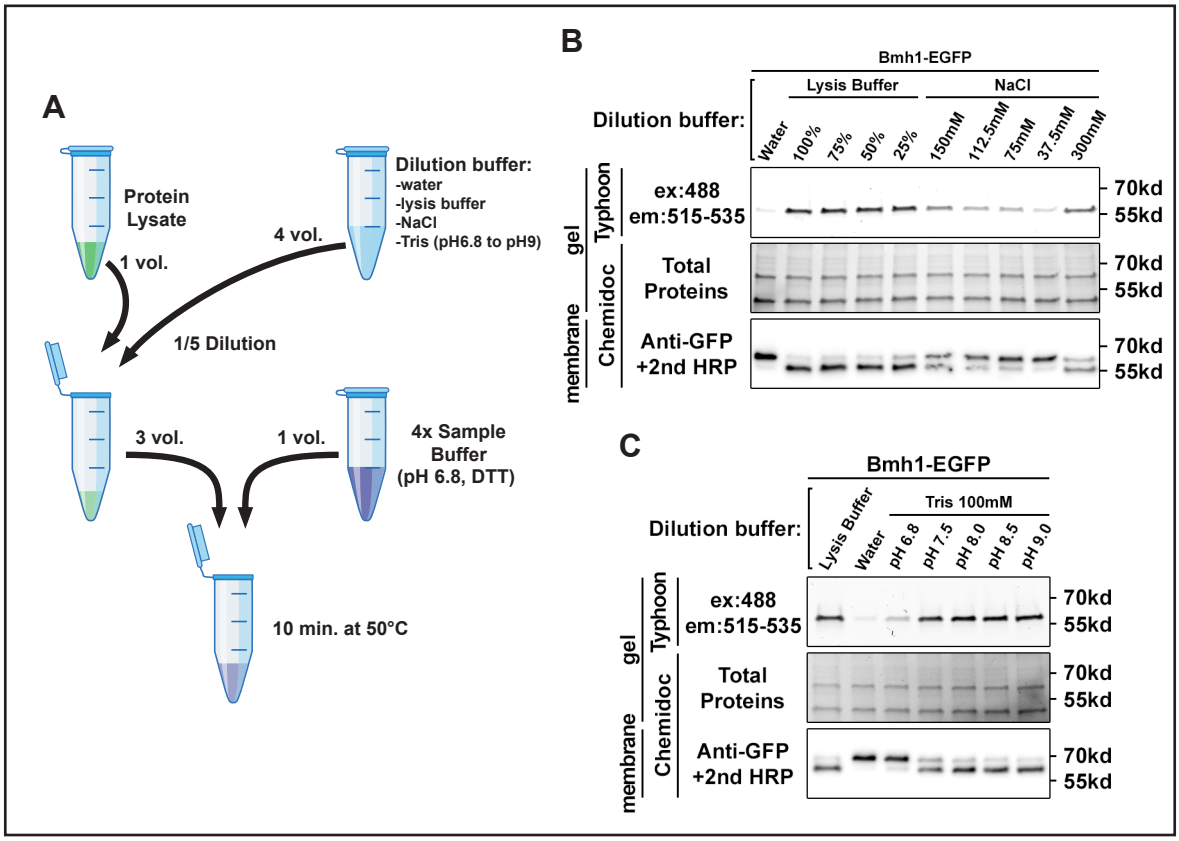
A
Protein Lysate
1 vol.
4 vol.
Dilution buffer:
-water
-lysis buffer
-NaCl
-Tris (pH6.8 to pH9)
1/5 Dilution
3 vol.
1 vol.
4x Sample Buffer (pH 6.8, DTT)
10 min. at 50°C
B
Bmh1-EGFP
Lysis Buffer
NaCl
Dilution buffer:
Water
100%
75%
50%
25%
150mM
112.5mM
75mM
37.5mM
300mM
gel
Typhoon
ex:488 em:515-535
membrane
Chemidoc
Total Proteins
Anti-GFP +2nd HRP
70kd
55kd
C
Bmh1-EGFP
Tris 100mM
Dilution buffer:
Lysis Buffer
Water
pH 6.8
pH 7.5
pH 8.0
pH 8.5
pH 9.0
gel
Typhoon
ex:488 em:515-535
membrane
Chemidoc
Total Proteins
Anti-GFP +2nd HRP
70kd
55kd

Figure 7

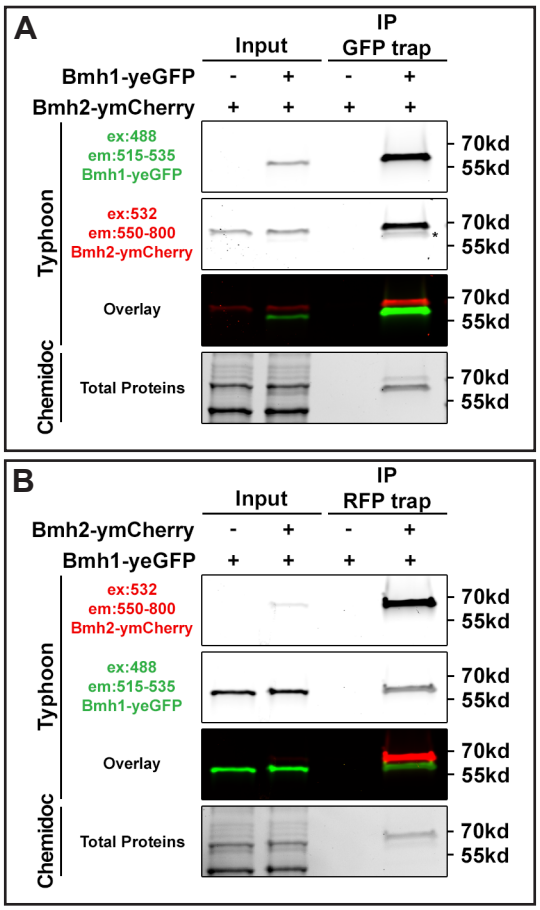
A
Input
IP
GFP trap
Bmh1-yeGFP
- + - +
Bmh2-ymCherry
+ + + +
Typhoon
ex:488
em:515-535
Bmh1-yeGFP
ex:532
em:550-800
Bmh2-ymCherry
Overlay
Chemidoc
Total Proteins
70kd
55kd
B
Input
IP
RFP trap
Bmh2-ymCherry
- + - +
Bmh1-yeGFP
+ + + +
Typhoon
ex:532
em:550-800
Bmh2-ymCherry
ex:488
em:515-535
Bmh1-yeGFP
Overlay
Chemidoc
Total Proteins
70kd
55kd

Figure 8

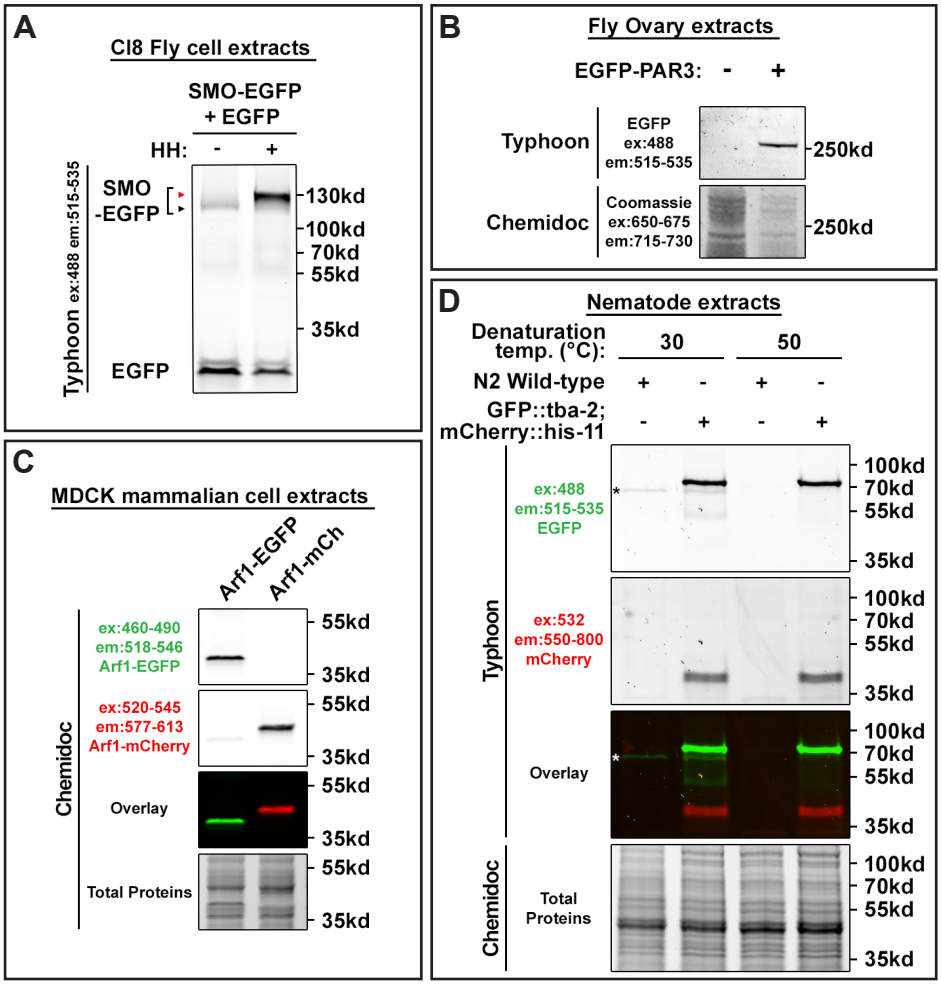
A
Cl8 Fly cell extracts
SMO-EGFP
+ EGFP
HH: - +
Typhoon ex:488 em:515-535
SMO
-EGFP
EGFP
130kd
100kd
70kd
55kd
35kd
B
Fly Ovary extracts
EGFP-PAR3: - +
Typhoon
EGFP
ex:488
em:515-535
250kd
Chemidoc
Coomassie
ex:650-675
em:715-730
250kd
C
MDCK mammalian cell extracts
Arf1-EGFP
Arf1-mCh
Chemidoc
ex:460-490
em:518-546
Arf1-EGFP
ex:520-545
em:577-613
Arf1-mCherry
Overlay
Total Proteins
55kd
35kd
D
Nematode extracts
Denaturation temp. (°C): 30 50
N2 Wild-type + - + -
GFP::tba-2; mCherry::his-11 - + - +
Typhoon
ex:488
em:515-535
EGFP
ex:532
em:550-800
mCherry
Overlay
Chemidoc
Total Proteins
100kd
70kd
55kd
35kd

Figure 9

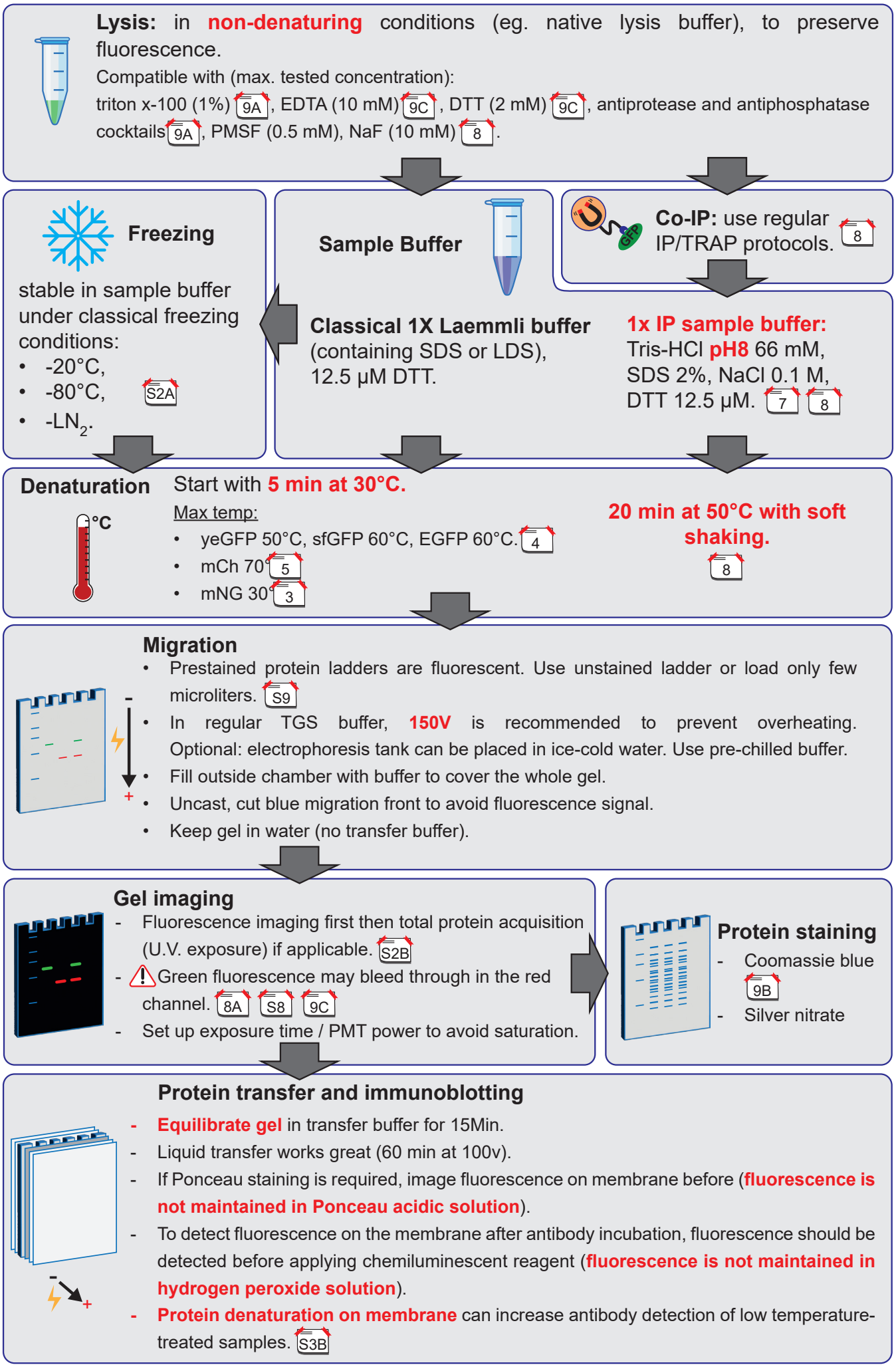
Lysis: in non-denaturing conditions (eg. native lysis buffer), to preserve fluorescence.
Compatible with (max. tested concentration):
triton x-100 (1%) 9A, EDTA (10 mM) 9C, DTT (2 mM) 9C, antiprotease and antiphosphatase cocktails 9A, PMSF (0.5 mM), NaF (10 mM) 8.
Freezing
stable in sample buffer under classical freezing conditions:
• -20°C,
• -80°C, S2A
• -LN2.
Sample Buffer
Classical 1X Laemmli buffer (containing SDS or LDS), 12.5 µM DTT.
Co-IP: use regular IP/TRAP protocols. 8
1x IP sample buffer:
Tris-HCl pH8 66 mM,
SDS 2%, NaCl 0.1 M,
DTT 12.5 µM. 7 8
Denaturation
°C
Start with 5 min at 30°C.
Max temp:
• yeGFP 50°C, sfGFP 60°C, EGFP 60°C. 4
• mCh 70° 5
• mNG 30° 3
20 min at 50°C with soft shaking.
8
Migration
• Prestained protein ladders are fluorescent. Use unstained ladder or load only few microliters. S9
• In regular TGS buffer, 150V is recommended to prevent overheating. Optional: electrophoresis tank can be placed in ice-cold water. Use pre-chilled buffer.
• Fill outside chamber with buffer to cover the whole gel.
• Uncast, cut blue migration front to avoid fluorescence signal.
• Keep gel in water (no transfer buffer).
Gel imaging
- Fluorescence imaging first then total protein acquisition (U.V. exposure) if applicable. S2B
- Green fluorescence may bleed through in the red channel. 8A S8 9C
- Set up exposure time / PMT power to avoid saturation.
Protein staining
- Coomassie blue 9B
- Silver nitrate
Protein transfer and immunoblotting
- Equilibrate gel in transfer buffer for 15Min.
- Liquid transfer works great (60 min at 100v).
- If Ponceau staining is required, image fluorescence on membrane before (fluorescence is not maintained in Ponceau acidic solution).
- To detect fluorescence on the membrane after antibody incubation, fluorescence should be detected before applying chemiluminescent reagent (fluorescence is not maintained in hydrogen peroxide solution).
- Protein denaturation on membrane can increase antibody detection of low temperature-treated samples. S3B

Figure 10

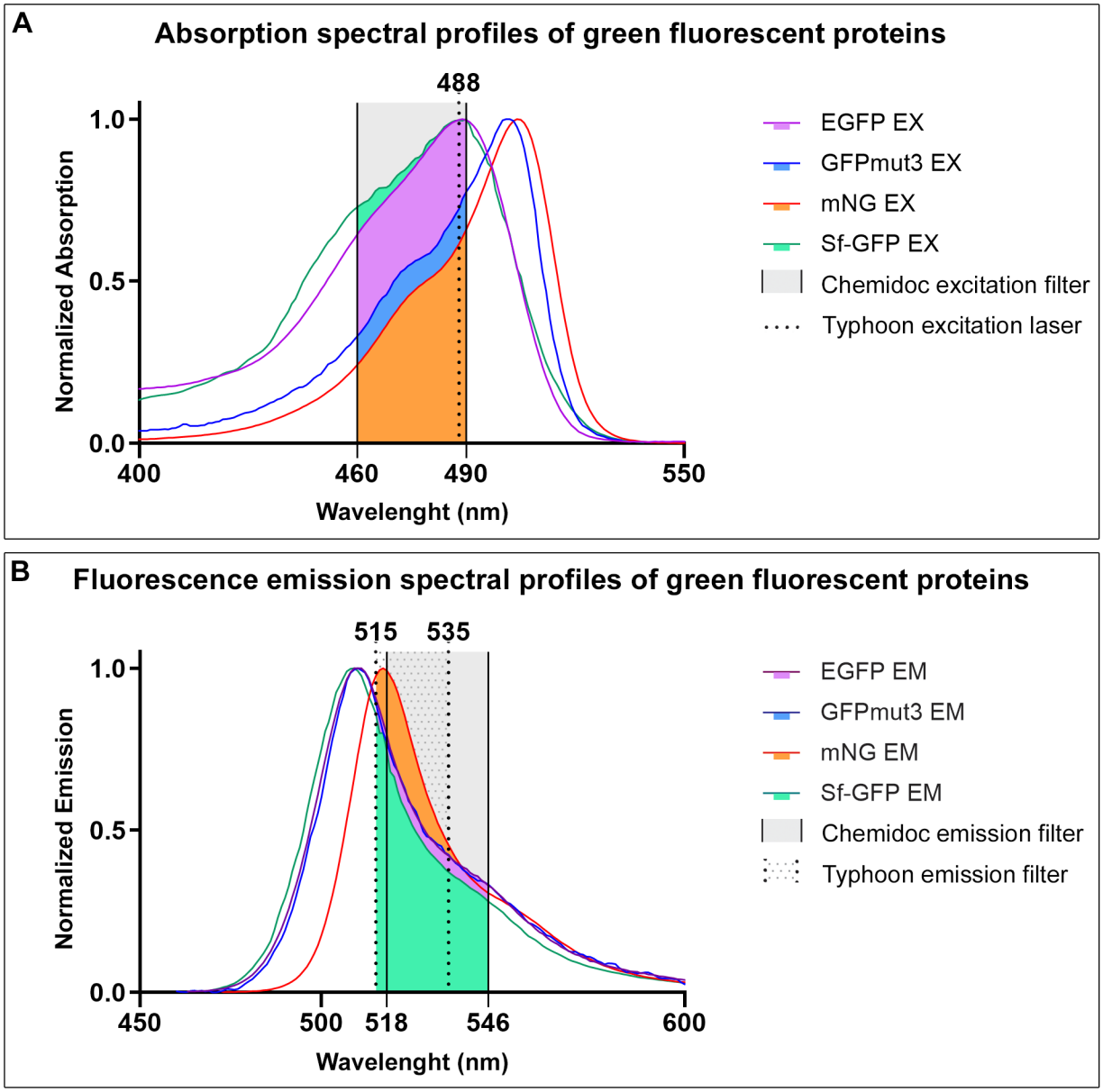
A
Absorption spectral profiles of green fluorescent proteins
488
1.0
0.5
0.0
Normalized Absorption
400
460
490
550
Wavelenght (nm)
EGFP EX
GFPmut3 EX
mNG EX
Sf-GFP EX
Chemidoc excitation filter
Typhoon excitation laser
B
Fluorescence emission spectral profiles of green fluorescent proteins
515
535
1.0
0.5
0.0
Normalized Emission
450
500
518
546
600
Wavelenght (nm)
EGFP EM
GFPmut3 EM
mNG EM
Sf-GFP EM
Chemidoc emission filter
Typhoon emission filter

Figure S1

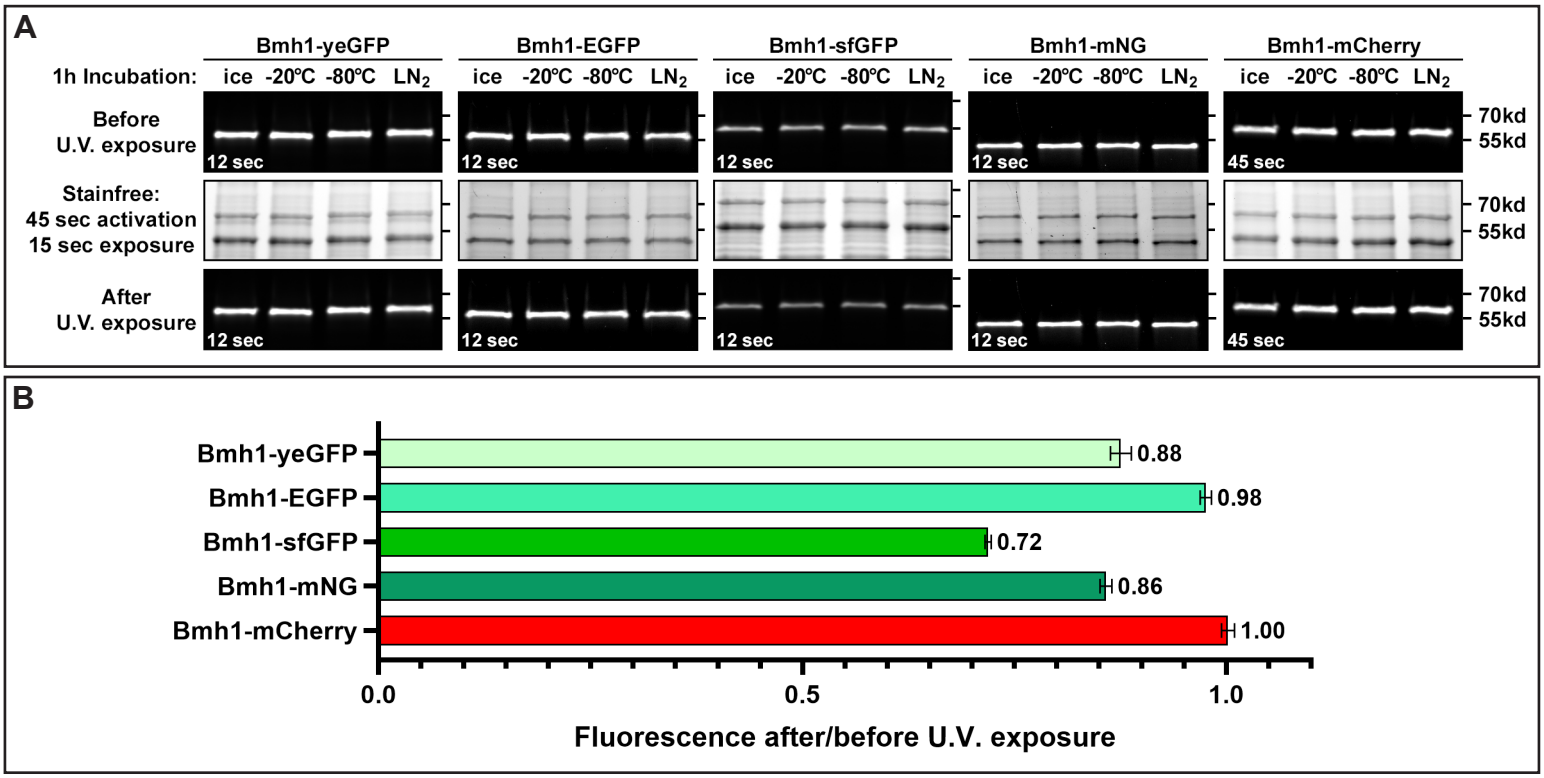
A
Bmh1-yeGFP
Bmh1-EGFP
Bmh1-sfGFP
Bmh1-mNG
Bmh1-mCherry
1h Incubation:
ice
-20°C
-80°C
LN2
Before U.V. exposure
Stainfree: 45 sec activation 15 sec exposure
After U.V. exposure
12 sec
45 sec
70kd
55kd
B
Bmh1-yeGFP
Bmh1-EGFP
Bmh1-sfGFP
Bmh1-mNG
Bmh1-mCherry
0.88
0.98
0.72
0.86
1.00
0.0
0.5
1.0
Fluorescence after/before U.V. exposure

Figure S2

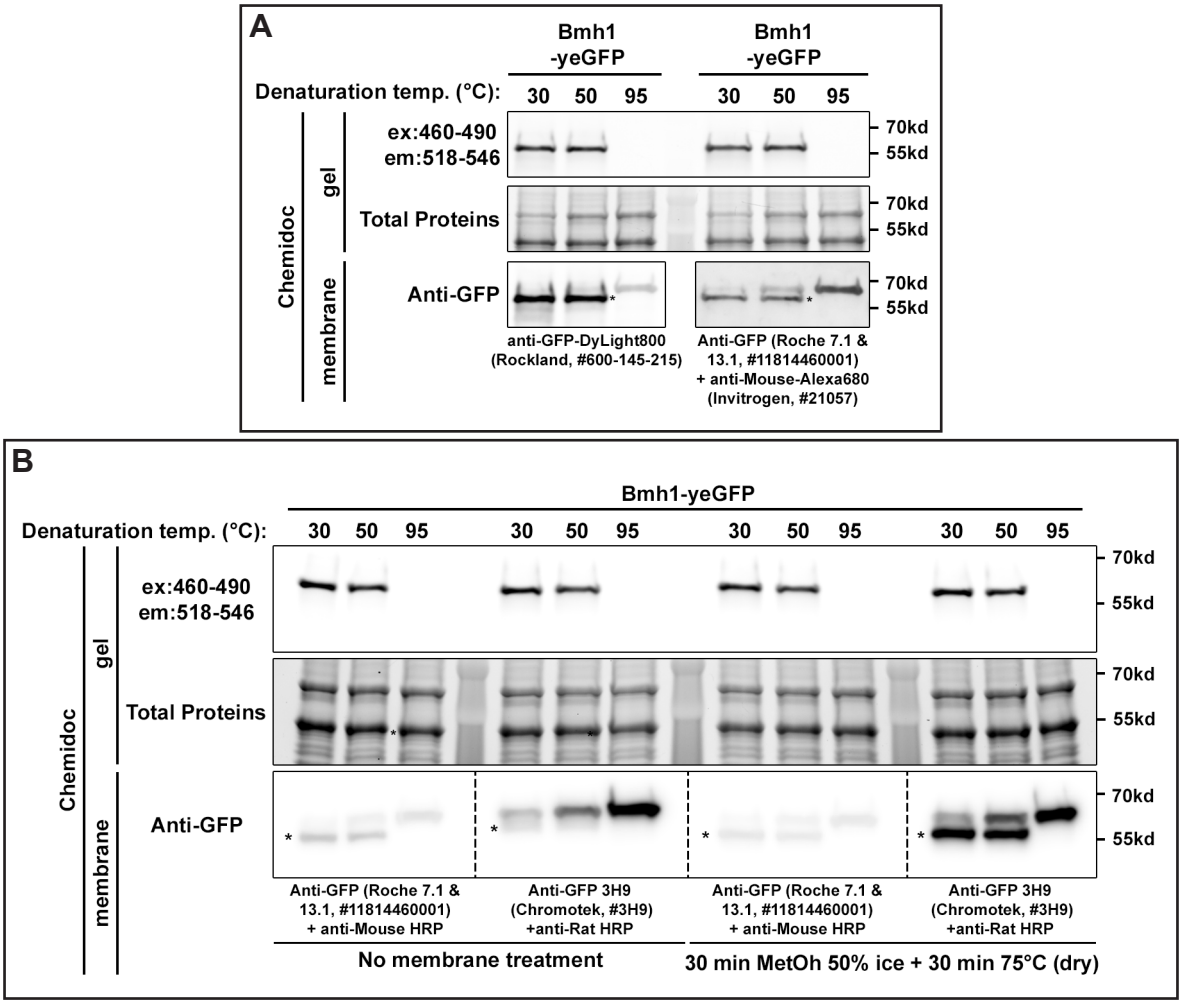
A
Bmh1 -yeGFP
Bmh1 -yeGFP
Denaturation temp. (°C):
30 50 95
30 50 95
Chemidoc
gel
membrane
ex:460-490 em:518-546
Total Proteins
Anti-GFP
70kd
55kd
anti-GFP-DyLight800 (Rockland, #600-145-215)
Anti-GFP (Roche 7.1 & 13.1, #11814460001) + anti-Mouse-Alexa680 (Invitrogen, #21057)
B
Bmh1-yeGFP
Denaturation temp. (°C):
30 50 95 30 50 95 30 50 95 30 50 95
Chemidoc
gel
membrane
ex:460-490 em:518-546
Total Proteins
Anti-GFP
70kd
55kd
Anti-GFP (Roche 7.1 & 13.1, #11814460001) + anti-Mouse HRP
Anti-GFP 3H9 (Chromotek, #3H9) +anti-Rat HRP
Anti-GFP (Roche 7.1 & 13.1, #11814460001) + anti-Mouse HRP
Anti-GFP 3H9 (Chromotek, #3H9) +anti-Rat HRP
No membrane treatment
30 min MetOh 50% ice + 30 min 75°C (dry)

Figure S3

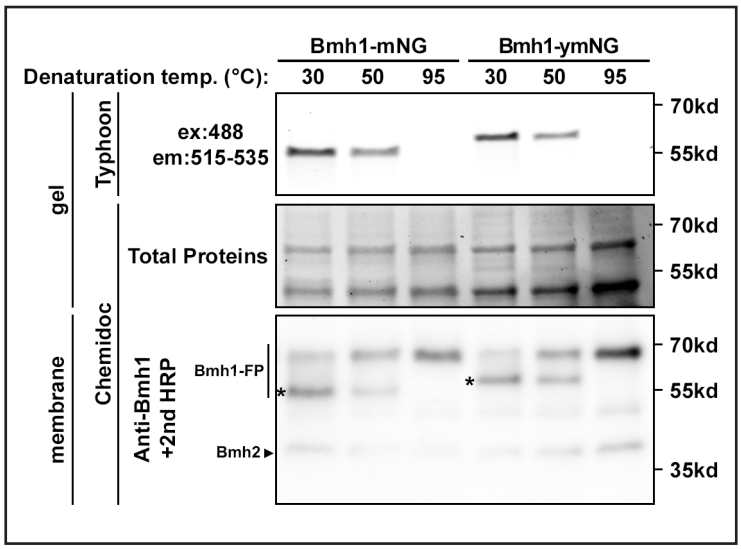
Bmh1-mNG
Bmh1-ymNG
Denaturation temp. (°C):
30
50
95
30
50
95
gel
Typhoon
ex:488
em:515-535
70kd
55kd
Chemidoc
Total Proteins
70kd
55kd
membrane
Anti-Bmh1
+2nd HRP
Bmh1-FP
*
*
Bmh2
70kd
55kd
35kd

Figure S4

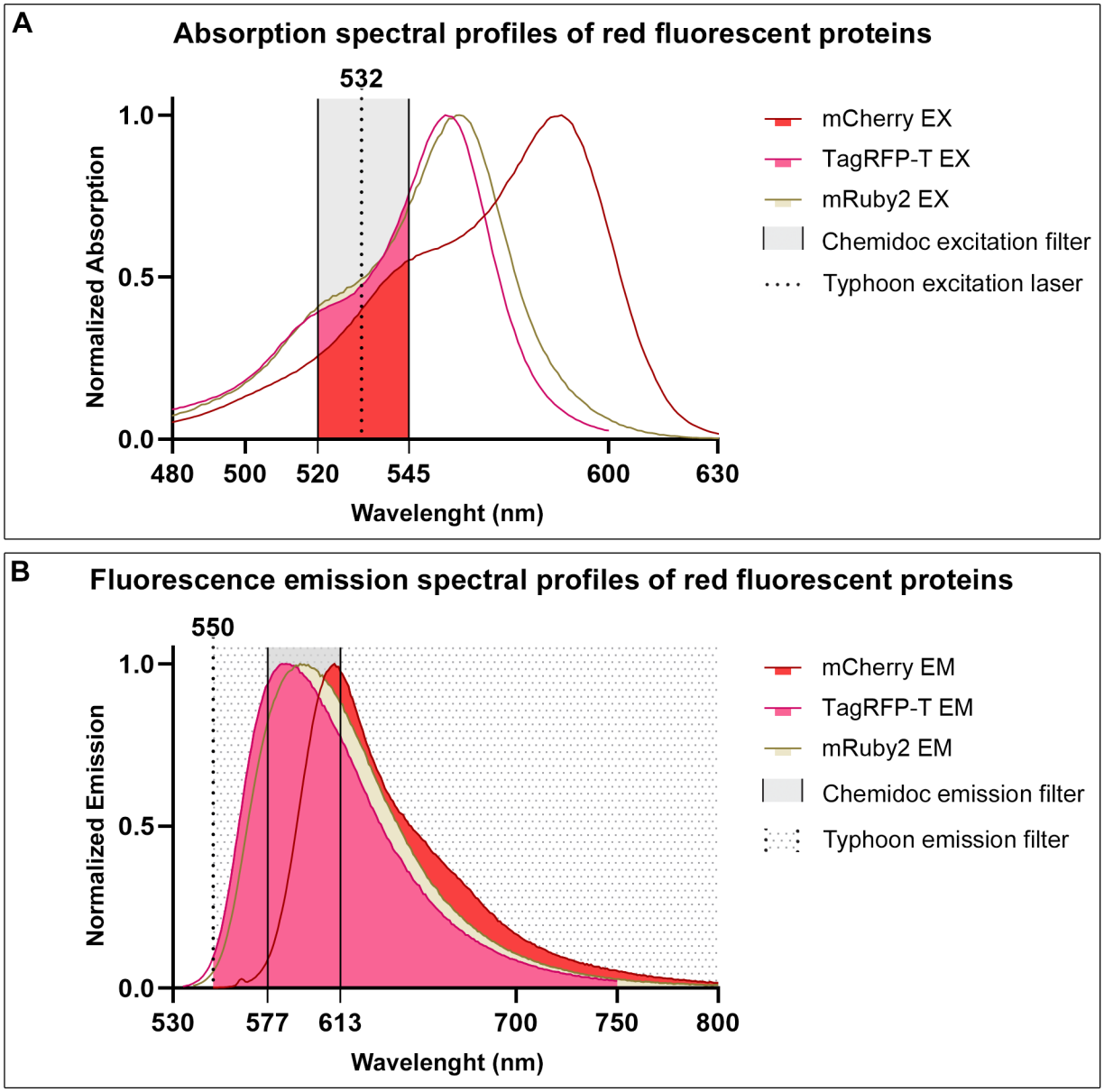
A
Absorption spectral profiles of red fluorescent proteins
532
1.0
0.5
0.0
Normalized Absorption
480
500
520
545
600
630
Wavelenght (nm)
mCherry EX
TagRFP-T EX
mRuby2 EX
Chemidoc excitation filter
Typhoon excitation laser
B
Fluorescence emission spectral profiles of red fluorescent proteins
550
1.0
0.5
0.0
Normalized Emission
530
577
613
700
750
800
Wavelenght (nm)
mCherry EM
TagRFP-T EM
mRuby2 EM
Chemidoc emission filter
Typhoon emission filter

Figure S5

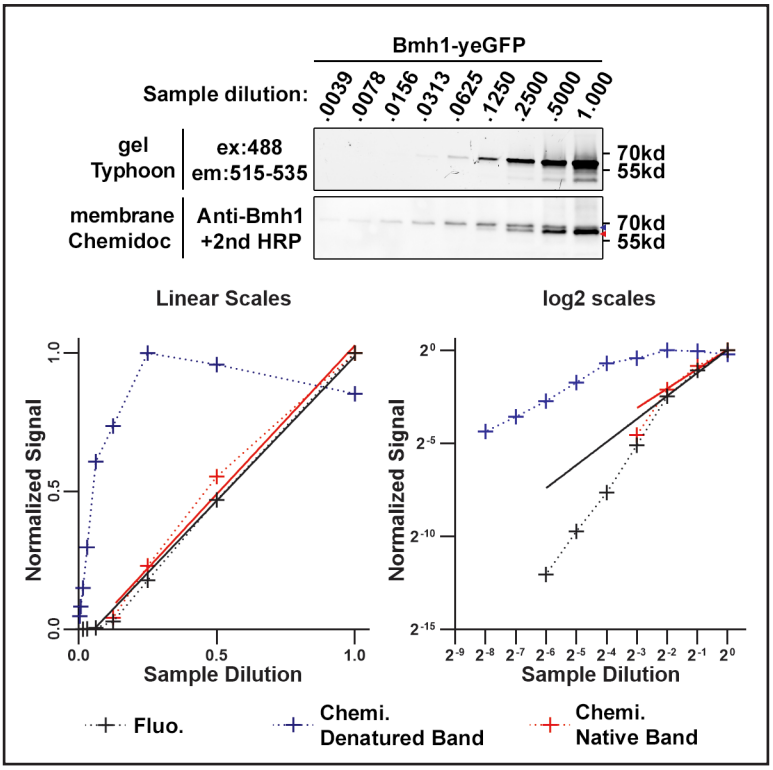
Bmh1-yeGFP
Sample dilution:
.0039
.0078
.0156
.0313
.0625
.1250
.2500
.5000
1.000
gel
Typhoon
ex:488
em:515-535
70kd
55kd
membrane
Chemidoc
Anti-Bmh1
+2nd HRP
70kd
55kd
Linear Scales
log2 scales
Normalized Signal
Sample Dilution
Normalized Signal
Sample Dilution
Fluo.
Chemi.
Denatured Band
Chemi.
Native Band

Figure S6

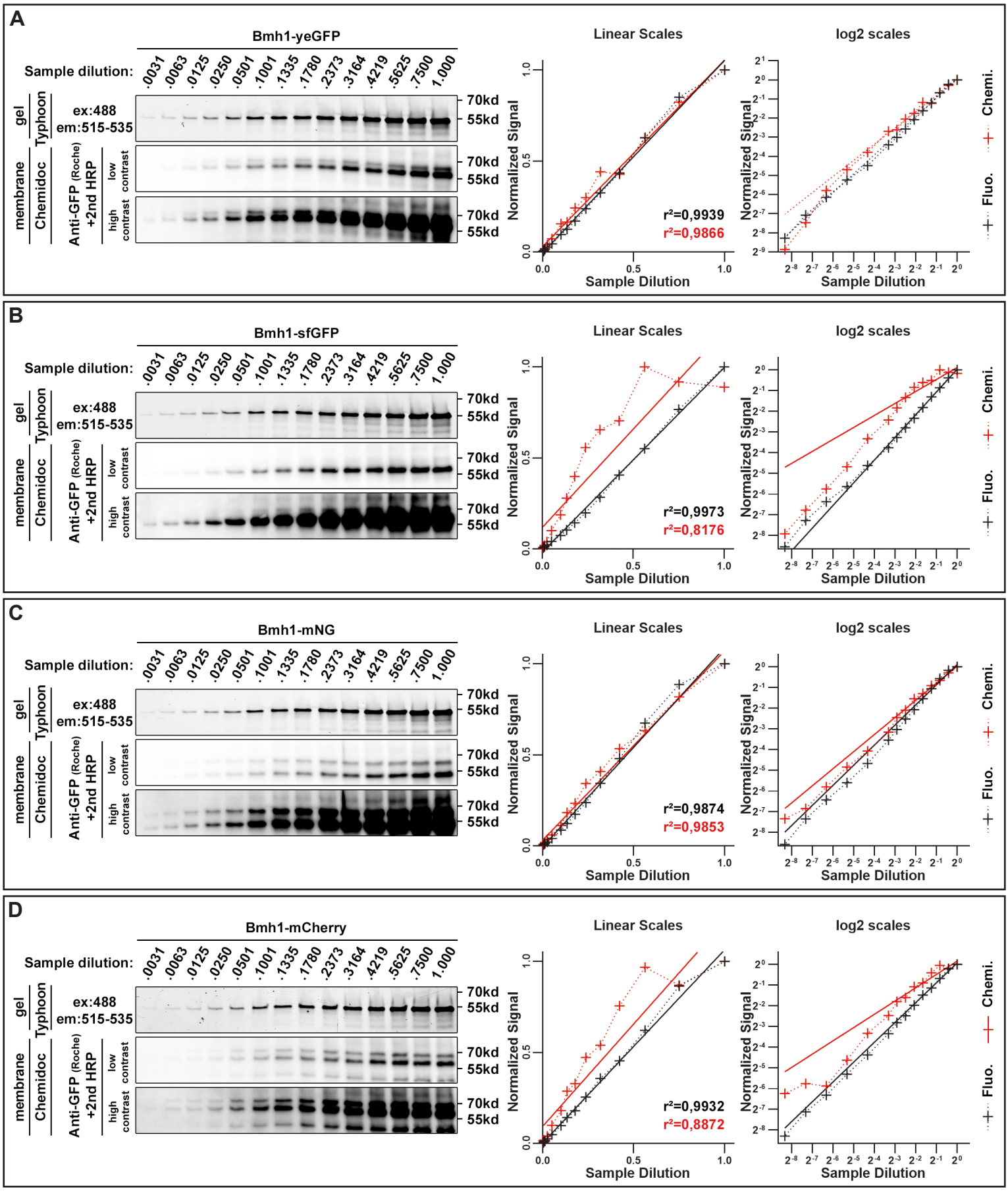
A
Bmh1-yeGFP
Sample dilution:
.0031 .0063 .0125 .0250 .0501 .1001 .1335 .1780 .2373 .3164 .4219 .5625 .7500 1.000
gel
Typhoon
ex:488
em:515-535
membrane
Chemidoc
Anti-GFP (Roche)
+2nd HRP
low contrast
high contrast
70kd
55kd
Linear Scales
log2 scales
Normalized Signal
Sample Dilution
r²=0,9939
r²=0,9866
Chemi.
Fluo.
B
Bmh1-sfGFP
r²=0,9973
r²=0,8176
C
Bmh1-mNG
r²=0,9874
r²=0,9853
D
Bmh1-mCherry
r²=0,9932
r²=0,8872

Figure S7

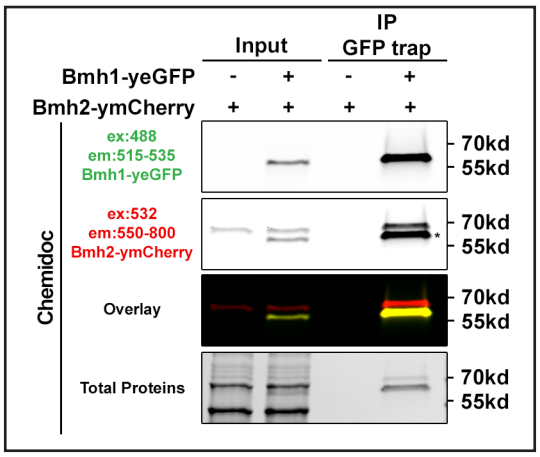
Input
IP
GFP trap
Bmh1-yeGFP
- + - +
Bmh2-ymCherry
+ + + +
Chemidoc
ex:488
em:515-535
Bmh1-yeGFP
ex:532
em:550-800
Bmh2-ymCherry
Overlay
Total Proteins
70kd
55kd
70kd
55kd
70kd
55kd
70kd
55kd
*

Figure S8

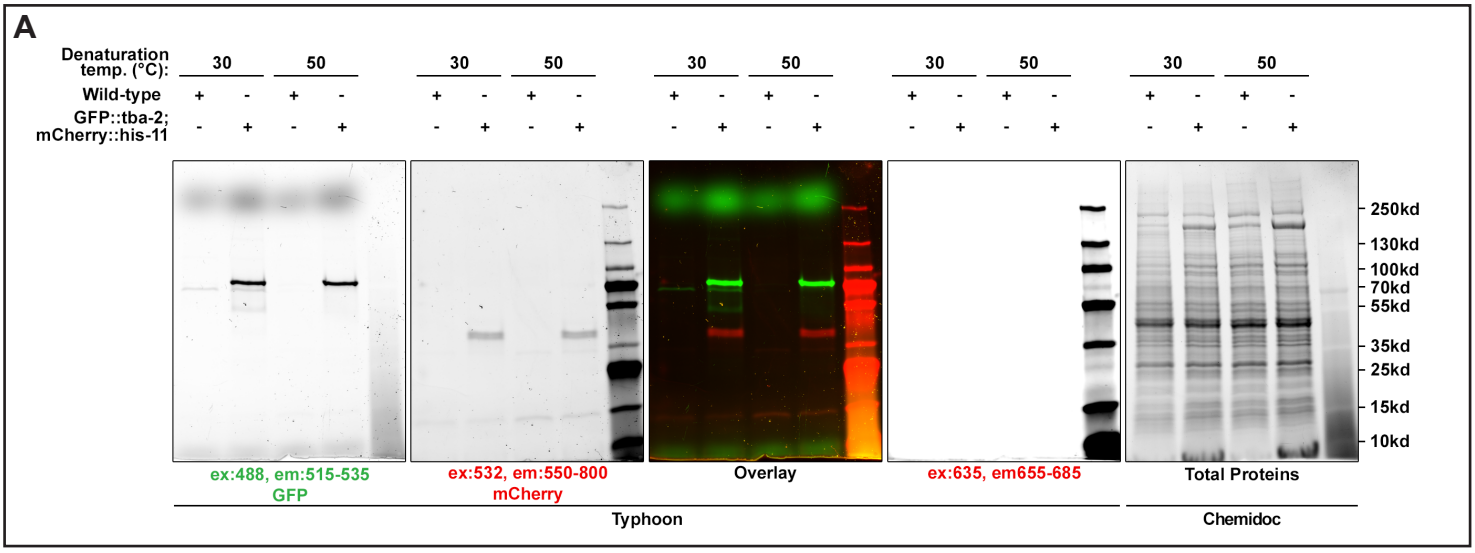
A
Denaturation temp. (°C):
30
50
Wild-type
GFP::tba-2; mCherry::his-11
250kd
130kd
100kd
70kd
55kd
35kd
25kd
15kd
10kd
ex:488, em:515-535
GFP
ex:532, em:550-800
mCherry
Overlay
ex:635, em655-685
Total Proteins
Typhoon
Chemidoc

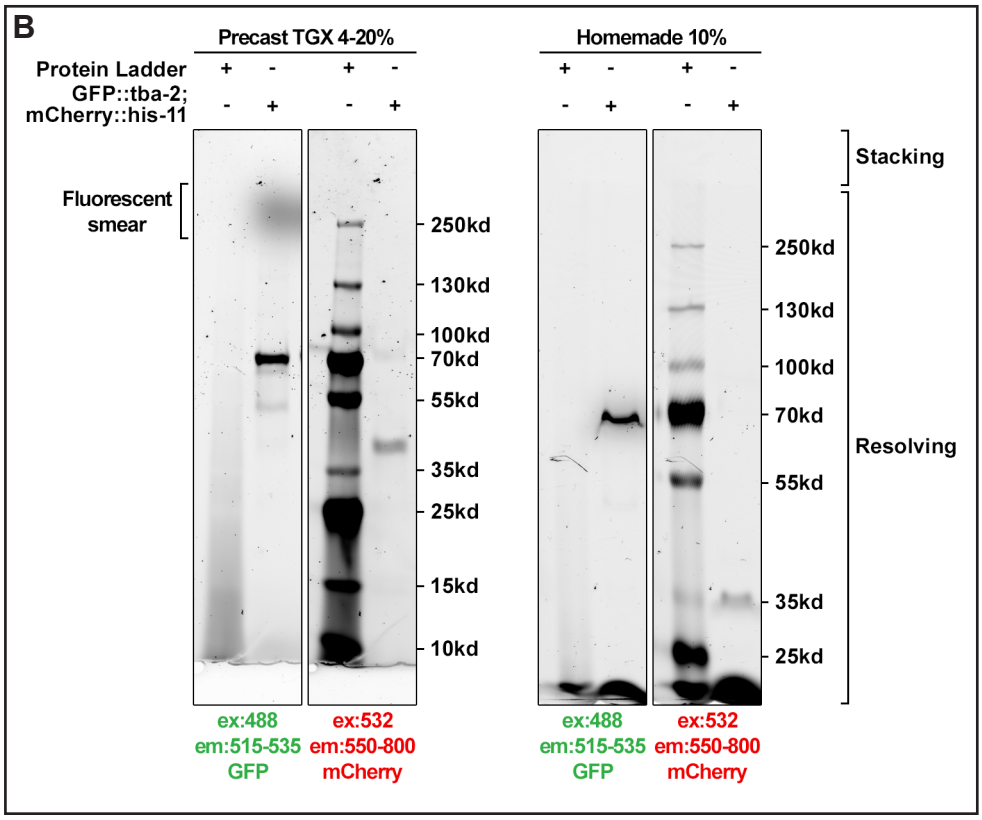
B
Precast TGX 4-20%
Homemade 10%
Protein Ladder
GFP::tba-2; mCherry::his-11
Fluorescent smear
Stacking
Resolving
250kd
130kd
100kd
70kd
55kd
35kd
25kd
15kd
10kd
ex:488
em:515-535
GFP
ex:532
em:550-800
mCherry

Figure S9